

Comparison of the bony labyrinth (inner ear) of extinct and extant hedgehogs (Eulipotyphla, Mammalia) and their effect on previously established phylogenetic trees

Flora M. van Glabbeek

Abstract

Although many scientists have studied the phylogeny of the Erinaceidae and have perceived the living and fossil groups to be near-relatives; the relationships, especially between extant and extinct species, are still tangled. This research is conducted in order to clarify the erinaceid phylogeny based on a combination of morphological and molecular data, while at the same time applying the new information on the bony labyrinth. This has resulted in the first detailed description of the bony labyrinth of the Erinaceidae, including the extinct genus *Postpalerinaceus* and *Parasorex*. This description provides new anatomical data that was used in the reconstruction of a phylogenetic tree. The trees based only on the bony labyrinth of extant species give a clear distinction between Erinaceinae and Galericinae. However, when fossils are included, some positions of the species are counter-intuitive as the extinct Erinaceinae genus *Amphexinus* is placed among the Galericinae. At the same time, the extinct Galericinae genus *Parasorex* is placed in the middle of the Erinaceinae clade. Nevertheless, the general pattern of genera remains the same, no matter what data source (e.g. DNA, morphology, the bony labyrinth) or species (extinct or extant) are used. Based on this finding, it can be concluded that the bony labyrinth is a trustworthy characteristic for determining Erinaceidae on genus level. In order to specify on species level more data is necessary.

Introduction

Among the many morphological characteristics researched on mammals one of the most neglected is probably the inner ear (bony labyrinth). Together with the outer (pinna and external auditory meatus) and middle ear (malleus, incus and stapes) these three parts make up the entire ear and function as the receiver, converter and transmitter of sound (Ekdale, 2013; Jeffrey and Spoor, 2004; Meng and Fox, 1995; Spoor and Zonneveld, 1998; Stieger et al., 2006) as well as the balancing organ (Billet et al., 2012; Ekdale and Rowe, 2011; Ekdale, 2013; Gunz et al., 2012; Jeffrey and Spoor, 2004; Pacholke et al., 2005; Spoor and Zonneveld, 1998). Although there is no doubt regarding the importance of the hearing organ, the location in the skull makes it problematic to analyze. The outer and even part of the middle ear are visible from the outside, but the inner ear is placed deep within the skull, which makes the bony labyrinth impossible to measure without opening

and thereby damaging the materials. This destructive type of research made broad comparisons of the inner ear scarce (Fleisher 1973; Gray, 1906, 1907, 1908; Hyrtl, 1845), especially when rare extinct material was concerned. However, thanks to rapid developments in modern technology, the use of the micro CT-scan is becoming more common and allows the inner ear to be visualised without doing any permanent damage on extant (Billet et al., 2012; Ekdale, 2010; Ekdale and Rowe, 2011; Gunz et al., 2012) as well as on extinct species (Georgi et al., 2013; Marugan-Lobon et al, 2013). It was not until recently that the bony labyrinth has gradually become more important in the description of the species and well researched families, where the inner ear previously was not included for other characteristics, e.g. the family Erinaceidae. The addition of the bony labyrinth to the species morphological description will help the phylogenetic relationships within

this family getting one step closer to a resolution.

The phylogeny of the Erinaceidae family, consisting of the subgroups Erinaceinae (spiny hedgehogs) and Galericinae (hairy hedgehogs, often referred to as moonrats) has been the subject of many debates. Even though there have been many studies on the phylogenetic relationships within the family, several problems still remain due to many discoveries of new paraphyletic groups. Previous studies have focused on either extant forms (Corbet, 1988; Frost et al., 1991) or fossil taxa (Novacek et al., 1985; Rich, 1981). The latter is made possible by an extensive fossil record (Figure 1), with genera dating back to the late Eocene (Butler, 1948; Villier and Carnevale, 2013; Ziegler et al., 2007)

The first study that combined both recent and fossil data in a phylogenetic tree was Gould (1995). Her results gave a new interpretation of the relationships between fossils and with living taxa. This intensive study covered all species of Erinaceidae and was an important step towards resolving relationships in the family. In a

later study, Gould (2001) openly doubted the usefulness of the dental characteristics, which formed the major part of the fossil dataset. The critical position of Gould towards dental characteristics is in sharp contrast with the palaeontological literature on erinaceids, which heavily depends on these characteristics. Naturally, palaeontologists have recognized these limitations, particularly within the spiny hedgehogs (Ziegler, 2005). Even now, there is still some debate concerning the gymnures, e.g. the genera *Parasorex*, *Schizogalerix* and *Galerix* (Doukas and van den Hoek Ostende, 2006; van den Hoek Ostende, 2001), which were formerly classified as the single genus *Galerix* (Butler, 1980). Although they are now differentiated from each other, the phylogenetic relationships within the genera are still vague, leading to much disagreement among scientists (Butler, 1980; Doukas and van den Hoek Ostende, 2006; Engesser, 1980; van den Hoek Ostende, 2001; Prieto et al., 2011, 2012; Ziegler, 2005).

Figure 1 The stratigraphic distribution of the various genera of the Erinaceidae.

Epoch	Stage	MA (from)	<i>Ampechinus</i>	<i>Atelerix</i>	<i>Brachyerix</i>	<i>Echinorex</i>	<i>Erinaceus</i>	<i>Galerix</i>	<i>Hemiechinus</i>	<i>Hylomys</i>	<i>Lantanoherium</i>	<i>Metechinus</i>	<i>Mesechinus</i>	<i>Mioechinus</i>	<i>Neohylomys</i>	<i>Neotetracus</i>	<i>Neurogymnurus</i>	<i>Paraechinus</i>	<i>Parasorex</i>	<i>Podogymnura</i>	<i>Postpalerhinaceus</i>
Holocene		0.00																			
Pleistocene		0.01																			
Miocene	Piacenzian	2.59																			
	Zanclian	3.60																			
	Messinian	5.33																			
	Tortonian	7.25																			
	Serravallian	11.61																			
	langhian	13.65																			
Oligocene	Burdigian	15.97																			
	Aquitanian	20.43																			
	Chatthian	23.03																			
Eocene	Rupelian	28.4																			
	Priabonian	33.9																			
	Bartonian	37.2																			

However, disagreement in relation to the use of fossils in the reconstruction of the phylogenetic tree is not limited to the family Erinaceidae (Grantham, 2004). Of course, the use of fossils can lead to a number of voids in a dataset, since the majority of fossils are fragments of an entire skeleton. In incomplete fossils, many traits are poorly preserved (Patterson, 1981), which gives a limited view on the characteristics used for comparisons. Therefore the use of incomplete fossils would always be inferior to extant data. Patterson even went as far as to state that the inclusion of fossils would not be beneficial to any phylogenetic tree produced, since the one-sidedness of the characteristics could lead to false conclusions in the underlying species relationships.

Despite the limitations associated with working with fossils, their importance in sampling across geological time is obvious, and they often comprise key taxa in breaking “long branches.” Donoghue (1989) explains that in many cases “long branches” do not result from anagenetic changes of an ancestral lineage, but rather from only a few species surviving from a particular clade. When apomorphic characters from such a lineage are examined they are often removed as they are considered to be uninformative, since the entire clade with these characters have become extinct apart from a sole survivor. By removing these characters, valuable information gets lost. However, when extinct species are included, such characters can play an important part in positioning taxa, to the extent that they can even reposition the former terminal taxon. Perhaps the most important reasons to adding fossils to the dataset is because, despite all its flaws, a fossil is another taxa within the clade and a denser sampling leads to more accurate results (Smith, 1998). With the importance of fossils in mind, the most comprehensive attempt to reconstruct the Erinaceid family was with a

combination of morphological and molecular datasets (He et al., 2012). Depending on the analysis, they used between 14 and 24 specimens of erinaceid for their phylogenetic trees, excluding the outgroups produced an impressive number of trees, of all different combinations, i.e. DNA only, morphology only or a combination of both. However, even the most inclusive tree still had some uncertainties, e.g., the node encompassing *Atelerix*, *Erinaceus* and *Paraechinus*. He et al. suggest that this was due to a posterior assignment of missing data, such as DNA or the inclusion of taxa with too few informative morphological characters (e.g. in *Hylomys parvus*, characters were taken from the literature which resulted in missing data for 71 characters out of a one 135 character matrix). These are all valid explanations for the voids that still remain, however it should be noted that the use of incomplete data in literature studies does not differ very much from the use of incomplete data from fossils. It seems strange that the former is widely accepted while the latter is frowned upon. The study of He et al. (2012) did not contain any extinct species even though the family of Erinaceidae has a well-documented fossil record (Butler, 1956, 1980, 1984; van den Hoek Ostende, 2001; Prieto et al., 2011, 2012 Villier et al., 2013). In order to bridge the gap between extant and extinct species, this paper will explore a middle ground to examine the bony labyrinth in both recant and fossil material.

Material and Methodology

Studied data

The specimens of Erinaceidae are stored in the collections of the Naturalis Biodiversity Centre (NBC) in Leiden, the University Museum of Zoology Cambridge (UMZC), the Naturhistorische Museum Wien (NMW) in Vienna, the Museo Nacional de Ciencias Naturales (MNCN) in Madrid and the Museum für Naturkunde (ZMB) in Berlin (Appendix table 1). In total 32 scans were made, representing 26

species of Erinaceidae and three additional scans of *Setifer setosus*, *Solenodon cubanus* and *Talpa europaeus* were made to serve as an outgroup (Appendix table 1). From the 26 Erinaceidae species and 3 outgroup species 14 were scanned in the NBC and 3 in the MNCN. The remaining 15 scans were made prior to the research and generously provided by; the UMZC which contributed 1 Erinaceidae scan and the 3 outgroups, the NMW which contributed 10 scans of Erinaceidae and the contribution of 4 scans from the ZMB. The constructed matrices from Gould (1995, 2001) were combined and added to this matrix in order to include species of which a scan could not be made. Since both matrixes of Gould showed some overlap in data, only a selection of each matrix was used (Appendix table 2).

CT-scans and 3D modelling

The skulls from the NBC collection (Appendix table 1) were scanned with a Skyscan 1172, the skulls from the NMB and the NMW collections were scanned with a Skyscan 1173. It is unknown which scanner types were used for the collections from the MNCN, the UMZC and the ZMB. Both sides of the skull were scanned, but only the right side was used for further analysis, since present differences between bony labyrinth characters on left and right sides are minor (Spoor and Zonneveld, 1998). The only exception to this rule was *Amphechinus edwardsi* NMB_SAUS_1, in which only the left inner ear was preserved. All scans were reconstructed using the program Mimics v15.0, a software by Materialise for processing 3D images. Together with the program ImageJ 25 characteristics of the bony labyrinth were measured (Figure 1 and 2)

DNA strands

The DNA material used by He et al. (2012) was stored on the website GENbank, which provided open access. In their study the material of 20 specimens (Appendix

table 3) and 3.177 mitochondrial base pairs were sequenced on the regions of 12S rRNA, Cytochrome B and NADH dehydrogenase subunit 2. The sequences were downloaded from GENbank and aligned within the program Bioedit Sequence Alignment Editor v7.1.9. Multiple sequences for one species were merged within the program Mesquite 2.75.

Phylogenetic analyses

The morphological character matrices from Gould (1995, 2001), the aligned DNA sequences and the bony labyrinth characteristic were combined into one overarching matrix within the program Mesquite. The final database was further analyzed within the program PAUP*4.0b10 through the use of the maximum parsimony as a criteria to create a phylogenetic tree (Swofford, 2003). All trees were made using majority rule consensus analysis with 1000 replications and with random additional sequence.

Bony labyrinth characters

The bony labyrinth was divided into 25 different characteristics to measure. To enable comparison between the species in spite of the variation in size, all characteristics within this matrix are measured in percentages or ratios.

1. Percentage of common crus (CC) length relative to the total bony labyrinth length (Lbl): (0) the CC% less than 30% of the total Lbl; (1) the CC% between 30% and 40% of total Lbl; (2) the CC% between 40% and 50% of total Lbl; (3) the CC% greater than 50% of total Lbl. The bony labyrinth was placed with the lateral semicircular canal in plane (Figure 2.A), to measure both the length of the total bony labyrinth and the common crus length. The former was measured by drawing a line from the top edge of the anterior semicircular canal towards the furthest outer posteriventral point of the cochlea (Spoor and Zonneveld, 1995) and the latter by drawing a midline through the

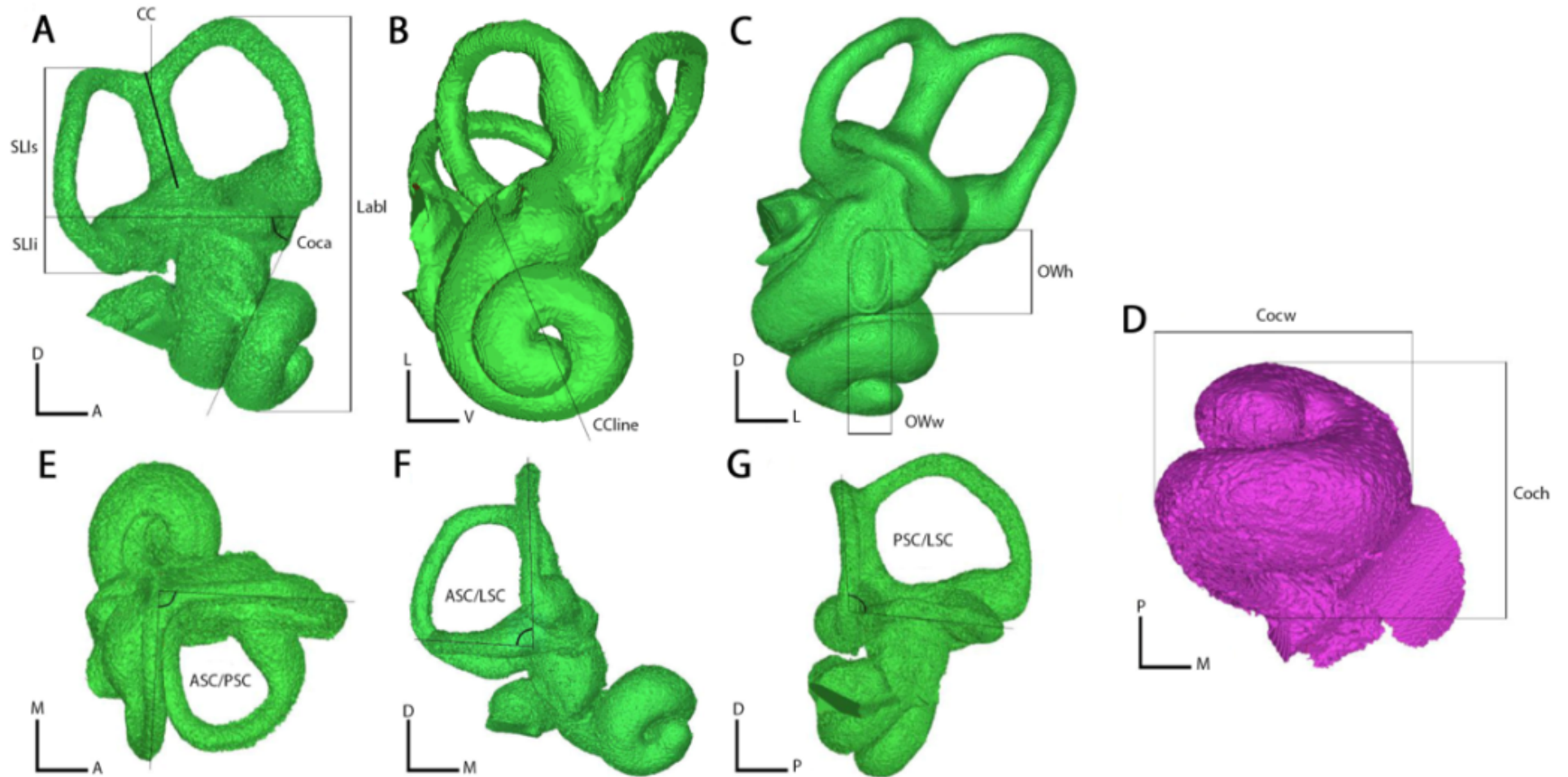


Figure 2 Measurements taken from the bony labyrinth. CocA, angle of the Cochlea; OWh, oval window height; OWw, oval window width; LabL, Labyrinth length; SLIs, Sagittal labyrinth index inferior; SLIs sagittal labyrinth index superior; ASC/PSC, the angle between the anterior- and posterior semicircular canals; ASC/LSC, the angle between the anterior- and lateral semicircular canals; PSC/LSC, the angle between the posterior- and lateral semicircular canals; Coch, Cochlea height; Cocw, Cochlea width. The micro CT-scan reconstructions are based on *Erinaceus europaeus* ZMA.86/4 (Figure 1.A, D, E, F), NMB.7008 (Figure 1.B) and *Paraechinus hylomylas* NMW.15242 (Figure 1.C).

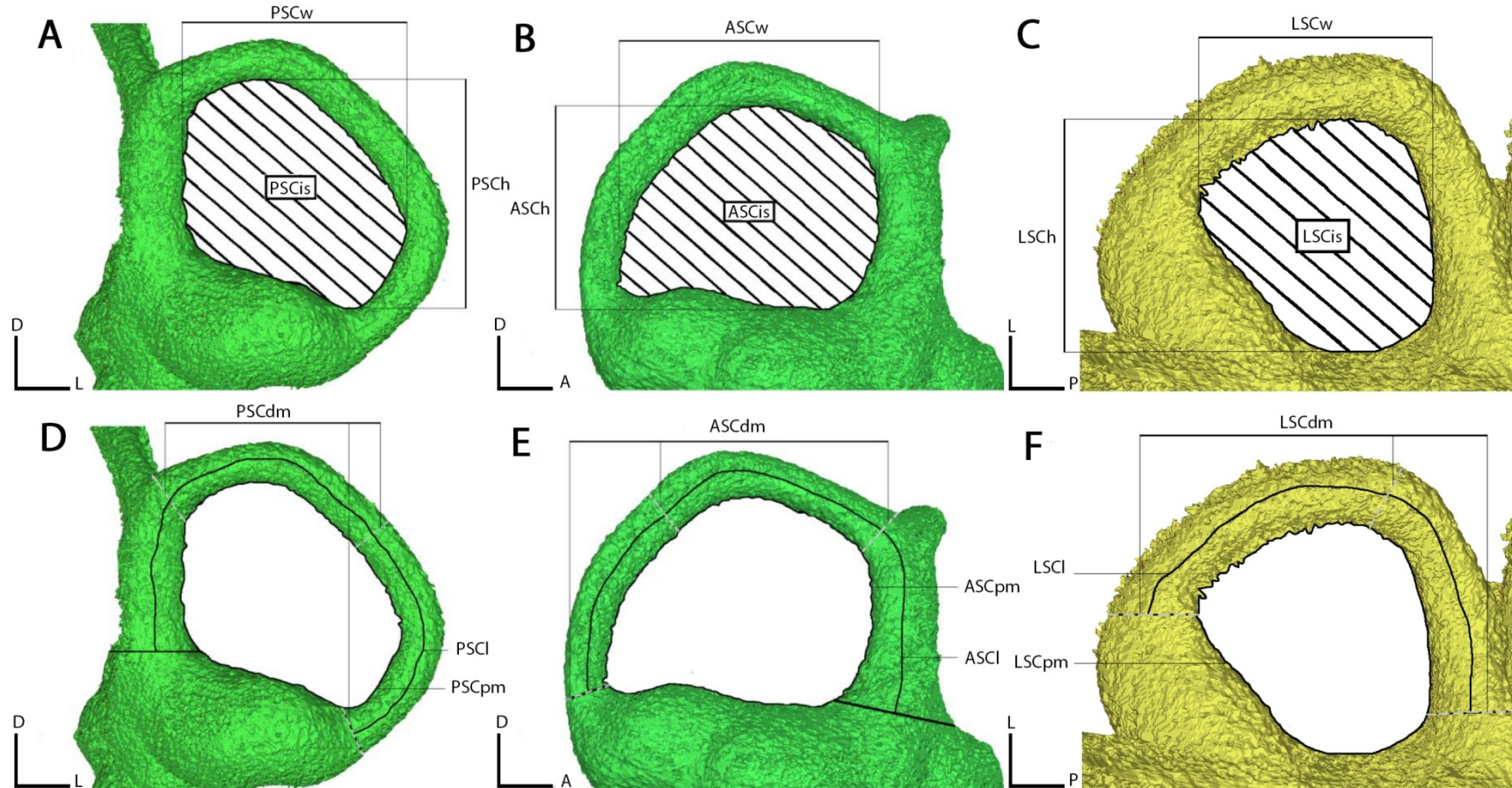


Figure 3 Measurements taken from the semicircular canals of the bony labyrinth. PSCh, Posterior semicircular canal height; PSCw, Posterior semicircular canal width; PSCdm, Posterior semicircular canal, diameter; PSCl, posterior semicircular canal length; PSCis, Posterior semicircular isosurface; PSCpm, posterior semicircular canal perimeter; ASCh, Anterior semicircular canal height, ASCw, Anterior semicircular canal width; ASCdm, Anterior semicircular canal diameter; ASCL, Anterior semicircular canal length; ASCis, Anterior semicircular canal isosurface; ASCpm, Anterior semicircular canal perimeter; LSCh, Lateral semicircular canal height; LSCw, Lateral semicircular canal width; LSCdm, Lateral semicircular canal diameter; LSCl, Lateral semicircular canal length; LSCis, Lateral semicircular canal isosurface; LSCpm, Lateral semicircular perimeter. The micro CT-scan reconstructions are based on *Erinaceus europaeus* ZMA.86/4 (Figure 2.A, B, C D, E, F).

CC, which starts between the anterior semicircular canal and the posterior semicircular canal until the CC meets at the base (Meng and Fox, 1995; Werner 1933). The percentage of the CC length relative to the total inner ear length is calculated by the formula below.

$$CC\% = \frac{CC \text{ length (mm)}}{\text{bony labyrinth total length (mm)}} * 100\%$$

2. The percentage of the cochlea canal volume (Cocv) relative to the total bony labyrinth volume (Labv): (0) The Cocv is less than 40% of the Labv; (1) The Cocv is between 40% and 50% of the Labv; (2) The Cocv is between 50% and 60% of the Labv; (3) The Cocv is greater than 60% of the Labv. This ratio is between the cochlea canal volume (mm³), cut from the ventral end of the fenestra vestibuli (oval window) and the entire volume (mm³) of the reconstructed labyrinth (Ekdale, 2013). The cochlea canal was placed in dorsal view for the measurement of the Cocv and Labv in Mimics (Figure 2.E and 2.D).

3. The angle of the cochlea canal is measured between; the first and second coil of the cochlea and a line straight through the lateral semicircular canal in plane view. Both lines are extended in order for them to meet and form an angle. The bony labyrinth was placed in lateral view in Mimics (Figure 2.A), while ImageJ was used to take measurements based on print screens from Mimics.

4. The numbers of coils in the cochlea canal (Coc): (0) less than 1 ½ coils; (1) between 1½ and 2 coils; (2) more than 2 coils. The cochlea canal was placed in posterior view in Mimics (Figure 2.B). This picture was uploaded in ImageJ where a straight line was drawn between the starting point of the cochlea canal and the ending of the oval window towards the axis of rotation of the cochlea canal (West, 1985). Every time the Coc crossed the line, it was counted as half a turn.

5. The shape index (SI) of the cochlea canal (Coc): (0) “flat”, with a SI value below 0.90; (1) “round”, with a SI value

between 0.90 and 1.10; (2) “sharp” with a SI value greater than 1.10. The cochlea canal (Coc) was placed in dorsal view in Mimics (Figure 2.D), and uploaded in ImageJ to measure both the height and width of the Coc. The height (mm) of the Coc was defined as the greatest vertical distance between the lateral edge and the oval window towards the apex (Ekdale and Rowe, 2011; Spoor and Zonneveld, 1995), while the width (mm) of the Coc was defined as the greatest horizontal distance between the anterior edge of the oval window and the opposite side of the Coc (Ekdale 2013; Ekdale and Rowe, 2011; Gosselin-Ildari, 2006; Spoor and Zonneveld, 1995). In Ekdale (2013), the shape index (SI) of the cochlea canal was calculated by dividing the Coc height by the Coc width. Ekdale made a distinction between the “flat” and “sharp” Coc depending on the value of the SI being less or higher than 0.55 respectively. However, these guidelines seemed to be inappropriate for this database as all the SI values were far above the value of 0.55. In order to fit the data better, three new categories were made.

6. The shape index (SI) of the oval window (OW): (0) the SI is less than 1.25; (1) the SI is between 1.25 and 1.50; (2) the SI is between 1.50 and 1.75; (3) the SI is greater than 1.75. The bony labyrinth was placed in lateral view in Mimics, with the oval window (OW) perpendicular in sight (Figure 2.C). Both the height (mm) and the width (mm) of OW were measured in ImageJ for the greatest vertical and horizontal distance between OW edges respectively (Meng and Fox, 1995). The shape index of the OW was calculated by dividing the height by the width.

7. The radius of curvature (RC) of the posterior semicircular canal (PSC): (0) the RC of the PSC is between 0.45 and 0.55; (1) the RC of the PSC is greater than 0.55. The bony labyrinth was positioned in posterior view in Mimics, with the posterior semicircular canal (PSC) in plane view (Figure 3.A). Within this position, the

PSC height (mm) and width (mm) were measured in ImageJ. The height is described as the greatest straight distance between the inner edge of the vestibule wall and the inner edge of the PSC lumen, while the width is defined as the greatest straight distance between the edge of the common crus and the edge of the PSC lumen (Ekdale, 2013; Jeffery and spoor, 2004; Spoor and Zonneveld, 1998). With both values, the radius of the curvature (RC) of the PSC can be calculated. However, in order to represent the RC in a percentage instead of an absolute number, the formula previously used was slightly adjusted.

$$\text{Old RC} = 0,5 * (\text{height} + \text{width}) / 2$$

$$\text{New RC} = (0,5 * ((\text{height} + \text{width}) / 2) / \text{height}) * 100$$

Initially there was also a group for a RC below 0.45. However, after the measurements no species seemed to have a RC equal or lower than 0.45. This category has therefore been removed.

8. The shape index (SI) of the posterior semicircular canal (PSC): (0) the SI of the PSC is less than 0.90; (1) the SI of the PSC is between 0.90 and 1.10; (2) the SI of the PSC is greater than 1.10. The bony labyrinth was positioned in posterior view in Mimics, with the posterior semicircular canal (PSC) in plane view (Figure 3.A). Within this position, the PSC height (mm) and width (mm) were measured in ImageJ. The height is described as the greatest straight distance between the inner edge of the vestibule wall and the inner edge of the PSC lumen, while the width is defined as the greatest straight distance between the edge of the common crus and the edge of the PSC lumen (Billet et al., 2012; Ekdale, 2013; Schmelzle and Villagra 2007; Spoor and Zonneveld, 1998).

9. The radius of curvature (RC) of the anterior semicircular canal (ASC): (0) the RC of the ASC is between 0.45 and 0.55;

(1) the RC of the ASC is greater than 0.55. The bony labyrinth was positioned in lateral view in Mimics, with the anterior semicircular canal (ASC) in plane view (Figure 3.B). Within this position, the ASC height (mm) and width (mm) were measured in ImageJ. The height is described as the greatest straight distance between the inner edge of the vestibule wall and the inner edge of the ASC lumen, while the width is defined as the greatest straight distance between the edge of the common crus and the edge of the ASC lumen (Ekdale, 2013; Spoor and Zonneveld, 1998). With both values, the radius of the curvature (RC) of the ASC can be calculated (for details see characteristic 7).

10. The shape index (SI) of the anterior semicircular canal (ASC): (0) the SI of the ASC is less than 0.90; (1) the SI of the ASC is between 0.90 and 1.10; (2) the SI of the ASC is greater than 1.10. The inner ear was positioned in lateral view in Mimics, with the anterior semicircular canal (ASC) in plane view (Figure 3.B). Within this position, the ASC height (mm) and width (mm) were measured in ImageJ. The height is described as the greatest straight distance between the inner edge of the vestibule wall and the inner edge of the ASC lumen, while the width is defined as the greatest straight distance between the edge of the common crus and the edge of the ASC lumen (Billet et al., 2012; Ekdale, 2013; Schmelzle and Villagra 2007; Spoor and Zonneveld, 1998).

11. The radius of curvature (RC) of lateral semicircular canal (LSC): (0) the RC of the LSC is between 0.45 and 0.55; (1) the RC of the LSC is greater than 0.55. The bony labyrinth was positioned in dorsal view in Mimics, with the lateral semicircular canal (LSC) in plane view (Figure 3.C). Within this position, the LSC height (mm) and width (mm) were measured in ImageJ. The height is described as the greatest straight distance between the inner edge of the vestibule wall and the inner edge of the LSC lumen,

while the width is defined as the greatest straight horizontal distance between the edges of the two LSC lumens (Ekdale, 2013; Spoor and Zonneveld, 1998). With these values, the radius of the curvature (RC) of the LSC can be calculated (for details see characteristic 7).

12. The shape index of the lateral semicircular canal: (0) the SI of the LSC is less than 0.90; (1) the SI of the LSC is between 0.90 and 1.10; (2) the SI of the LSC is greater than 1.10. The bony labyrinth was positioned in dorsal view in Mimics, with the lateral semicircular canal (LSC) in plane view (Figure 3.C). Within this position, the LSC height (mm) and width (mm) were measured in ImageJ. The height is described as the greatest straight distance between the inner edge of the vestibule wall and the inner edge of the LSC lumen, while the width is defined as the greatest straight horizontal distance between the edges of the two LSC lumens (Ekdale, 2013; Spoor and Zonneveld, 1998).

13. The angle between the anterior and posterior semicircular canal (ASC/PSC): (0) “acute angle,” an angle less than 85° ; (1) “right angle,” an angle between 85° and 95° ; (2) “obtuse angle,” an angle larger than 95° . The bony labyrinth was placed in dorsal view with both the anterior semicircular canal (ASC) and the posterior semicircular canal (PSC) perpendicular to the field of view (Ekdale, 2013) in Mimics. In cases where this placement was not possible, due to twists in either the ASC or the PSC, the inner ear was positioned in order to give an optimum (Figure 3.E). To compensate for the coils in the semicircular canals (SC), the midline through the SC was drawn based on nine points per SC; three points at the place where the common crus (CC) meets the CS (two on each side of the edge of the CC and one in the middle), three points in the middle of the SC (two on each side of the lumen edge and one in the middle of the lumen) and the last three at the far end of the SC. All the eighteen

points (nine for each SC) were placed in ImageJ, where coordinates were given. Based on the coordinates the program R calculated the best fitting line. The point at which both best fitting lines crossed, determined the degrees of the angle ASC/PSC.

14. The angle between the anterior and lateral semicircular canal (ASC/LSC): (0) “acute angle,” an angle less than 85° ; (1) “right angle,” an angle between 85° and 95° ; (2) “obtuse angle,” an angle larger than 95° . The bony labyrinth was placed in posterior view with both the anterior semicircular canal (ASC) and the lateral semicircular canal (LSC) perpendicular to the field of view (Ekdale, 2013) in Mimics. In cases where this placement was not possible, due to twists in either the ASC or the LSC, the inner ear was positioned in order to give an optimum (Figure 2.F). To compensate for the coils in the semicircular canals (SC), the midline through the SC was drawn based on two best fitting lines (for details see character 14). The point at which both best fitting lines crossed, determined the degrees of the angle ASC/LSC.

15. The angle between the posterior and lateral semicircular canal (PSC/LSC): (0) “right angle,” an angle between 85° and 95° ; (1) “obtuse angle,” an angle larger than 95° . The bony labyrinth was placed in lateral view with both the posterior semicircular canal (PSC) and the lateral semicircular canal (LSC) perpendicular to the field of view (Ekdale, 2013) in Mimics. In cases where this placement was not possible, due to twists in either the PSC or the LSC, the inner ear was positioned in order to give an optimum (Figure 2.G). To compensate for the coils in the semicircular canals (SC), the midline through the SC was drawn based on two best fitting lines (for details see character 14). The point at which both best fitting lines crossed, determined the degrees of the angle PSC/LSC.

16. The sagittal labyrinth index (SLI): (0) a SLI less than 10%; (1) a SLI between

10% and 20%; (2) a SLI between 20% and 30%; (3) a SLI greater than 30%. The bony labyrinth was placed in lateral view in Mimics (Figure 2.A). The sagittal labyrinth index (SLI) was calculated by measuring the percentage of the posterior semicircular canal (PSC) that is located inferior to that of the lateral semicircular canal (LSC). The part of the PSC above the LSC is known as the SLIs, whereas the part of the PSC below LSC is called SLIi (Spoor and Zonneveld, 1998; Jeffrey and Spoor, 2004). In ImageJ a straight line through the middle of the LSC was drawn, as was the vertical line that collected the outer top edge of the PSC lumen to the point where the vestibula and the PSC lumen meet.

17. The ratio of the anterior semicircular canal inner surface (ASCis) relative to the posterior semicircular canal inner surface (PSCis): (0) a ratio below 0,95 (PSCis is greater than ASCis); (1) a ratio between 0,95 and 1,05 (ASCis and PSCis are equal); (2) a ratio between 1,05 and 2,05 (ASCis is up to twice the size of PSCis); (3) a ratio greater than 2,05 (ASCis is more than two times greater than PSCis). The bony labyrinth was positioned in posterior view in Mimics, with the posterior semicircular canal (PSC) in plane view (Figure 3.A) in order to measure the PSC inner surface (PSCis). The entire area is surrounded by semicircular canals on one side to the common crus and by vestibula on the other side. The inner ear was positioned in anterior view in Mimics, with the anterior semicircular canal (ASC) in plane view (Figure 3.B) in order to measure the ASC inner surface (ASCis). The entire area is surrounded by semicircular canals on one side to the common crus and by vestibula on the other side. Both the ASCis and the PSCis were measured in ImageJ.

18. The ratio of the anterior semicircular canal inner surface (ASCis) relative to the lateral semicircular canal inner surface (LSCis): (0) a ratio below 0,95 (LSCis is greater than ASCis); (1) a ratio between 0,95 and 1,05 (ASCis and

LSCis are equal); (2) a ratio between 1,05 and 2,05 (ASCis is up to twice the size of LSCis); (3) a ratio greater than 2,05 (ASCis is more than two times greater than LSCis). The bony labyrinth was positioned in posterior view in Mimics, with the lateral semicircular canal (LSC) in plane view (Figure 3.C) in order to measure the LSC inner surface (LSCis). The entire area is surrounded by the LSC and the vestibula. The inner ear was positioned in anterior view in Mimics, with the anterior semicircular canal (ASC) in plane view (Figure 3.B) in order to measure the ASC inner surface (ASCis). The entire area is surrounded by semicircular canals on one side to the common crus and by vestibula on the other side. Both the ASCis and the LSCis were measured in ImageJ.

19. The ratio of the posterior semicircular canal inner surface (PSCis) relative to the lateral semicircular canal inner surface (LSCis): (0) a ratio below 0,95 (LSCis is greater than PSCis); (1) a ratio between 0,95 and 1,05 (PSCis and LSCis are equal); (2) a ratio between 1,05 and 2,05 (PSCis is up to twice the size of LSCis); (3) a ratio greater than 2,05 (ASCis is more than two times greater than LSCis). The inner ear was positioned in posterior view in Mimics, with the lateral semicircular canal (LSC) in plane view (Figure 3.C) in order to measure the LSC inner surface (LSCis). The entire area is surrounded by the LSC and the vestibula. The inner ear was positioned in anterior view in Mimics, with the anterior semicircular canal (PSC) in plane view (Figure 3.A) in order to measure the PSC inner surface (PSCis). Both the PSCis and the LSCis were measured in ImageJ.

20. The ratio of the anterior semicircular canal perimeter (ASCpm) relative to the posterior semicircular canal (PSCpm): (0) a ratio below 0,95 (PSCpm is greater than ASCpm); (1) a ratio between 0,95 and 1,05 (ASCpm and PSCpm are equal); (2) a ratio greater than 1,05 (ASCpm is greater than PSCpm). The bony labyrinth was positioned in posterior

view in Mimics, with the posterior semicircular canal (PSC) in plane view (Figure 3.D) in order to measure the PSC perimeter (PSCpm). The inner edge of the PSC, common crus and vestibula form the line of the PSCpm (Jones and Spells 1963; Cox and Jeffery 2010). The inner ear was positioned in posterior view in Mimics, with the anterior semicircular canal (ASC) in plane view (Figure 3.E) in order to measure the ASC perimeter (ASCpm). The inner edge of the ASC, common crus and vestibula formed the line of the ASCpm (Jones and Spells 1963; Cox and Jeffery 2010). The circumferences (were measured in ImageJ).

21. The ratio of the anterior semicircular canal perimeter (ASCpm) relative to the lateral semicircular canal perimeter (LSCpm): (0) a ratio below 0,95 (LSCpm is greater than ASCpm); (1) a ratio between 0,95 and 1,05 (ASCpm and LSCpm are equal); (2) a ratio greater than 1,05 (ASCpm is greater than LSCpm). The bony labyrinth was positioned in posterior view in Mimics, with the lateral semicircular canal (LSC) in plane view (Figure 3.F) in order to measure the LSC perimeter (LSCpm). The inner edge of the LSC and vestibula form the line of the LSCpm (Jones and Spells 1963; Cox and Jeffery 2010). The inner ear was positioned in posterior view in Mimics, with the anterior semicircular canal (ASC) in plane view (Figure 3.E) in order to measure the ASC perimeter (ASCpm). The inner edge of the ASC, common crus and vestibula formed the line of the ASCpm (Jones and Spells 1963; Cox and Jeffery 2010). The circumferences were measured in ImageJ.

22. The ratio of the posterior semicircular canal perimeter (PSCpm) relative to the lateral semicircular canal perimeter (LSCpm): (0) a ratio below 0,95 (LSCpm is greater than PSCpm); (1) a ratio between 0,95 and 1,05 (PSCpm and LSCpm are equal); (2) a ratio greater than 1,05 (PSCpm is greater than LSCpm). The bony labyrinth was positioned in posterior

view in Mimics, with the lateral semicircular canal (LSC) in plane view (Figure 3.F) in order to measure the LSC perimeter (LSCpm). The inner edge of the LSC and vestibula formed the line of the LSCpm (Jones and Spells 1963; Cox and Jeffery 2010). The inner ear was positioned in posterior view in Mimics, with the posterior semicircular canal (PSC) in plane view (Figure 3.D) in order to measure the PSC perimeter (PSCpm). The inner edge of the PSC, common crus and vestibula formed the line of the PSCpm (Jones and Spells 1963; Cox and Jeffery 2010). The circumferences were measured in ImageJ.

23. The ratio of the posterior semicircular canal length (PSCl) relative to the posterior semicircular canal diameter (PSCdm): (0) the PSCl is less than 15 times the length of the PSCdm; (1) the PSCl is between 15 and 30 times the length of the PSCdm; (2) the PSCl is between 30 and 45 times the length of the PSCdm; (3) the PSC is more than 45 times the PSCdm length. The inner ear was positioned in posterior view in Mimics, with the posterior semicircular canal (PSC) in plane view (Figure 3.D). The PSC length (PSCl) was measured by drawing a line in Mimics from the base of the common crus across the lumen up to (but excluding) the ampulle (Edkale, 2013). The PSC diameter (PSCdm) was measured in ImageJ by drawing a line across the PSC at three different places: at the border of the PSC and the common crus, in the middle between the common crus and the vestibule and at the border of the PSC and the vestibule. The PSCl was divided with the PSCdm in order to get the ratio.

24. The ratio of the anterior semicircular canal length (ASCl) relative to the anterior semicircular canal diameter (ASCDm): (0) the ASCl is less than 15 times the length of the ASCdm; (1) the ASCl is between 15 and 30 times the length of the ASCdm; (2) the ASCl is between 30 and 45 times the length of the ASCdm; (3) the ASC is more than 45

times the ASCdm length. The inner ear was positioned in anterior view in Mimics, with the anterior semicircular canal (ASC) in plane view (Figure 3.E). The ASC length (ASCl) was measured by drawing a line in Mimics from the base of the common crus across the lumen up to (but excluding) the ampulle (Edkale, 2013). The ASC diameter (ASCdm) was measured in ImageJ by drawing a line across the ASC at three different places: at the border of the ASC and the common crus, in the middle between the common crus and the vestibule and at the border of the ASC and the vestibule. The ASCl was divided with the ASCdm in order to get the ratio.

25. The ratio of the lateral semicircular canal length (LSCl) relative to the lateral

semicircular canal diameter (LSCdm): (0) the LSCl is less than 15 times the length of the LSCdm; (1) the LSCl is between 15 and 30 times the length of the LSCdm; (2) the LSCl is between 30 and 45 times the length of the LSCdm; (3) the ASC is more than 45 times the LSCdm length. The inner ear was positioned in lateral view in Mimics, with the lateral semicircular canal (LSC) in plane view (Figure 3.D). The LSC length (LSCl) was measured by drawing a line in Mimics from the base of the vestibuli across the lumen up to (but excluding) the ampulle (Edkale, 2013). The LSC diameter (LSCdm) was measured in ImageJ by drawing a line across the LSC at three different places: at the border of the LSC and the vestibuli, in the middle between the common crus and the vestibule and at the border of the LSC and the vestibule. The LSCl was divided with the LSCdm in order to get the ratio.

The results

Description of bony labyrinth

All the 32 scans of the bony labyrinth were used to make a description of the different genera of Erinaceidae. For every species used, one representative is given within the matrix with a general overview in the Appendix (Table 4).

Subgroup Erinaceinae

Genus *Amphechinus* (Figure 4)

Description (1) percentage of common crus length is between 30% and 40% of the total bony labyrinth length; (2) the percentage of the cochlea canal volume is between 50% and 60% of the total bony labyrinth volume; (3) the angle of the cochlea is greater than 45° ; (4) the cochlea canal coils between $1\frac{1}{2}$ and 2 times; (5) the shape index of the cochlea canal is greater than 0.90; (6) the shape index of the oval window is greater than 1.50; (7) the radius of curvature of the posterior semicircular canal is between 0.45 and 0.55; (8) the shape index of the posterior semicircular canal is less than 1.10; (9) the radius of curvature of the anterior

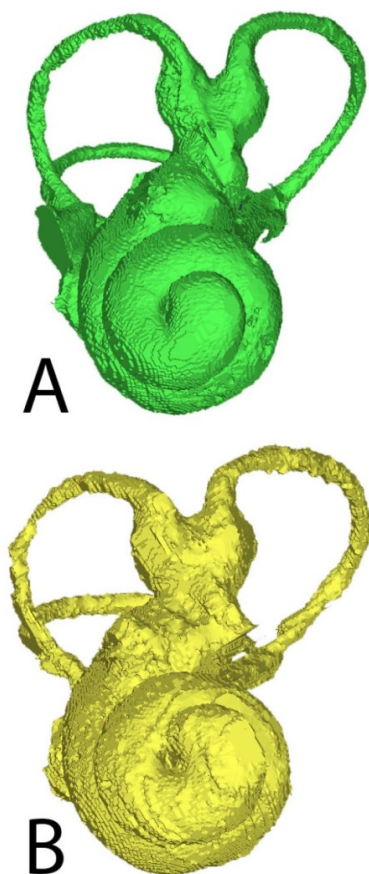


Figure 4 the bony labyrinth of the genus *Amphechinus* represented by A) *A. edwardsi* from NMB-SAUS_1 and B) *A. paleoedwardsi* from NMB-SAU_632

semicircular canal is greater than 0.45; (10) the shape index of the anterior semicircular canals is between 0.70 and 0.90; (11) the radius of curvature of the lateral canal is greater than 0.55; (12) the shape index of the lateral semicircular canal is between 0.70 and 0.90; (13) the angle between the anterior and posterior semicircular canal varies between “acute” and “right”; (14) the angle between the anterior and lateral semicircular canal varies between “right” and “obtuse”; (15) the angle between the posterior and lateral semicircular canals is “right”; (16) the sagittal labyrinth index is between 10% and 20%; (17) the ratio of the anterior relative to the posterior semicircular canal inner surface is between 1,05 and 2,05; (18) the ratio of the anterior relative to the lateral semicircular canal inner surface is between 0,95 and 1,05; (19) the ratio of the posterior relative to the lateral semicircular canal inner surface is between 0,95 and 2,05; (20) the ratio of the anterior relative to the posterior semicircular canal perimeter is greater than 1,05; (21) the ratio of the anterior relative to the lateral semicircular canal perimeter is greater than 1,05; (22) the ratio of the posterior relative to the lateral semicircular canal is less than 1,05; (23) the ratio of the posterior semicircular length is between 30 and 45 times greater than the posterior semicircular length; (24) the ratio of the anterior semicircular length is between 15 and 45 times greater than the anterior semicircular length; (25) the ratio of the lateral semicircular length is between 15 and 30 times greater than the lateral semicircular length.

Genus *Atelerix* (Figure 5)

Description_ (1) percentage of common crus length is between 30% and 40% of the total bony labyrinth length; (2) the percentage of the cochlea canal volume is between 40% and 50% of the total bony labyrinth volume; (3) the angle of the cochlea varied from less than 45° to greater than 55°; (4) the cochlea canal

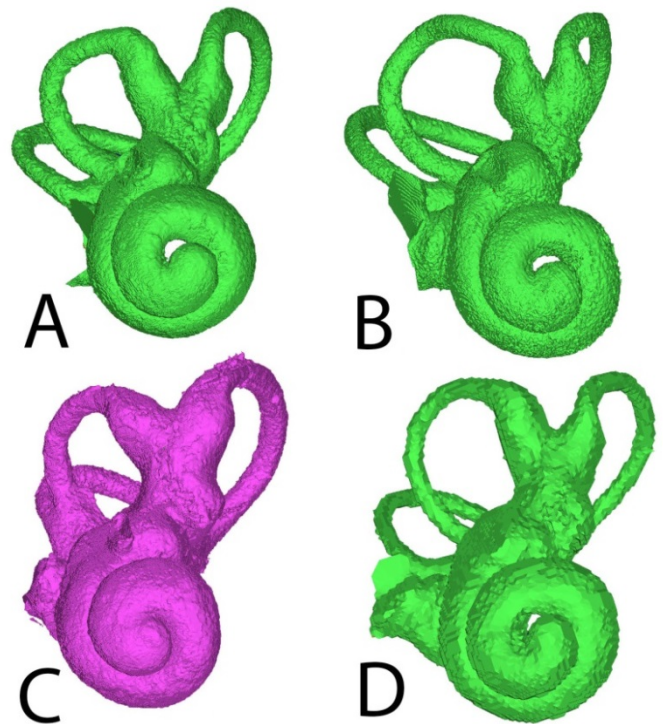


Figure 5 the bony labyrinth of the genus *Atelerix* represented by A) *A. albiventris* from NBC-RMNH.MAM.2518 B) *A. algirus* from NBC-RMNH.MAM.18759 C) *A. frontalis* from NBC- RMNH.MAM980 and D) *A. pruneri* from ZMB-MfN.60577

coils is less than 1 ½ times; (5) the shape index of the cochlea canal is less than 1.10; (6) the shape index of the oval window is found between 1.25 and 1.50 for all species with the exception of *A. frontalis* where the oval window had a shape index greater than 1.75; (7) the radius of curvature of the posterior semicircular canal is greater than 0.45; (8) the shape index of the posterior semicircular canal is less than 1.10; (9) the radius of curvature of the anterior semicircular canal is greater than 0.55; (10) the shape index of the anterior semicircular canals is less than 0.90; (11) the radius of curvature of the lateral canal is greater than 0.45; (12) the shape index of the lateral semicircular canal is between 0.70 and 0.90; (13) the angle between the anterior and posterior semicircular canals is “acute; (14) the angle between the anterior and lateral semicircular canal varies between “acute” and “right; (15) the angle between the posterior and lateral semicircular canals

varies from “acute” to “right”; (16) the sagittal labyrinth index is between 10% and 30%; (17) the ratio of the anterior relative to the posterior semicircular canal inner surface is less than 2,05; (18) the ratio of the anterior relative to the lateral semicircular canal inner surface is between 0,95 and 1,05; (19) the ratio of the posterior relative to the lateral semicircular canal inner surface less than 0,95 for all members of *Atelerix* with the exception of *A. frontalis*, which has a ratio of the posterior relative to the lateral semicircular canal inner face between 1,05 and 2,05; (20) the ratio of the anterior relative to the posterior semicircular canal perimeter varies from less than 0,95 for *A. algirus* to a value greater than 1,05 for *A. frontalis*; (21) the ratio of the anterior relative to the lateral semicircular canal perimeter is semicircular length is up to 30 times greater than the posterior semicircular

greater than 1,05; (22) the ratio of the posterior relative to the lateral semicircular canal is greater than 1,05 for all members of *Atelerix* with the exception of *A. frontalis*, which has a value less than 0,95; (23) the ratio of the posterior length; (24) the ratio of the anterior semicircular length is between 15 and 30 times greater than the anterior semicircular length; (25) the ratio of the lateral semicircular length is up to 15 greater than the lateral semicircular length.

Genus *Erinaceus* (Figure 6)

Description (1) percentage of common crus length is up to 40% of the total bony labyrinth length; (2) the percentage of the cochlea canal volume is less than 50% of the total bony labyrinth volume for all members of *Erinaceus* with the exception of *E. albiventris* which has a cochlea canal volume greater than 60% of the total bony labyrinth volume; (3) the angle of the cochlea is greater than 45°; (4) the cochlea canal has less than 1 ½ coils; (5) the shape index of the cochlea canal is less than 1.10; (6) the shape index of the oval window is between 1.25 and 1.75; (7) the radius of the curvature of the posterior semicircular canal is greater than 0.45; (8) the shape index of the posterior semicircular canal is less than 1.10; (9) the radius of curvature of the anterior semicircular canal is greater than 0.45; (8) the shape index of the posterior semicircular canal is less than 1.10; (9) the radius of curvature of the anterior semicircular canal is greater than 0.55; (10) the shape index of the anterior semicircular canals is less than 0.90; (11) the radius of curvature of the lateral canal is greater than 0.45; (12) the shape index of the lateral semicircular canal is between 0.70 and 0.90; (13) the angle between the anterior and posterior semicircular canal varies between “acute” and “right”; (14) the angle between the anterior and lateral semicircular canal varies between “acute” and “right”; (15) the angle between the posterior and lateral semicircular canals varies from “right” to

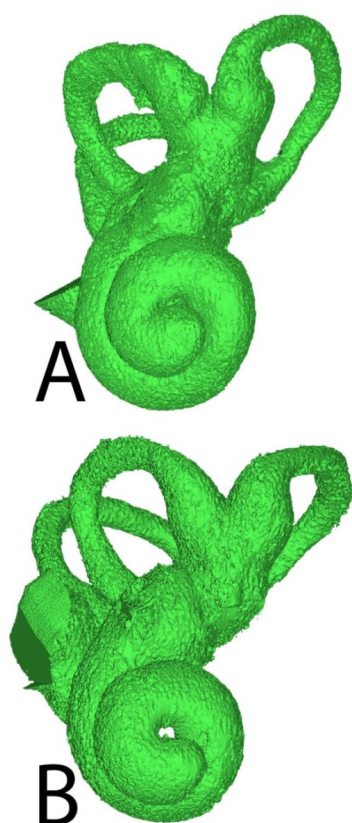


Figure 6 the bony labyrinth of the genus *Erinaceus* represented by A) *E. concolor* from NBC-ZMA.MAM.24943 B) *E. europeus* from NBC-ZMA.MAM.86/4

“obtuse”; (16) the sagittal labyrinth index is between 10% and 30%; (17) the ratio of the anterior relative to the posterior semicircular canal inner surface is between 0,95 and 2,05; (18) the ratio of the anterior relative to the lateral semicircular canal inner surface is between 0,95 and 2,05; (19) the ratio of the posterior relative to the lateral semicircular canal inner surface is greater than 1,05; (20) the ratio of the anterior relative to the posterior semicircular canal perimeter is greater than 0,95; (21) the ratio of the anterior relative to the lateral semicircular canal perimeter is greater than 1,05; (22) the ratio of the posterior relative to the lateral semicircular canal is less than 1,05; (23) the ratio of the posterior semicircular length is between 15 and 30 times greater than the posterior semicircular length; (24) the ratio of the anterior semicircular length is between 15 and 30 times greater than the anterior semicircular length; (25) the ratio of the lateral semicircular length is up to 15 times greater than the lateral semicircular length.

Genus *Hemiechinus* (Figure 7)

Description_ (1) percentage of common crus length is less than 30% of the total bony labyrinth length; (2) the percentage of the cochlea canal volume is between 40% and 50% of the total bony labyrinth volume; (3) the angle of the cochlea is between 45° and 55°; (4) the cochlea canal coils are between 1 ½ and 2 times; (5) the shape index of the cochlea canal is between 0.90 and 1.10; (6) the shape index of the oval window is between 1.50 and 1.75; (7) the radius of curvature of the posterior semicircular canal is between 0.45 and 0.55; (8) the shape index of the posterior semicircular canal is less than 0.70; (9) the radius of curvature of the anterior semicircular canal is greater than 0.55; (10) the shape index of the anterior semicircular canals is between 0.70 and 0.90; (11) the radius of curvature of the lateral canal is greater than 0.55; (12) the canal is between 0.70 and 0.90; (13) the angle between the anterior and posterior

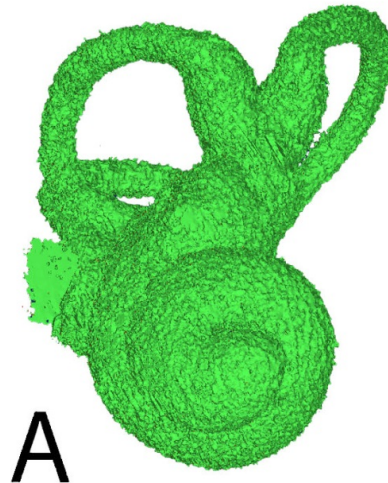


Figure 7 the bony labyrinth of the genus *Hemiechinus* represented by A) *H. auritus* from NBC-ZMA.MAM.1765

semicircular canals is “obtuse”; (14) the angle between the anterior and lateral semicircular canals is “acute”; (15) the angle between the posterior and lateral semicircular canals is “obtuse”; (16) the sagittal labyrinth index is between 20% and 30%; (17) the ratio of the anterior relative to the posterior semicircular canal inner surface is between 1,05 and 2,05; (18) the ratio of the anterior relative to the lateral semicircular canal inner surface is between 0,95 and 1,05; (19) the ratio of the posterior relative to the lateral semicircular canal inner surface is below 0,95; (20) the ratio of the anterior relative to the posterior semicircular canal perimeter is greater than 1,05; (21) the ratio of the anterior relative to the lateral semicircular canal perimeter is greater than 1,05; (22) the ratio of the posterior relative to the lateral semicircular canal is between 0,95 and 1,05; (23) the ratio of the posterior semicircular length is between 15 and 30 times greater than the posterior semicircular length; (24) the ratio of the anterior semicircular length is between 15 and 30 times greater than the anterior semicircular length; (25) the ratio of the lateral semicircular length is up to 15 times greater than the lateral semicircular length.

Genus *Mesechinus* (Figure 8)

Description_ (1) percentage of common crus length is between 30% and 40% of the total bony labyrinth length; (2) the percentage of the cochlea canal volume is between 40% and 50% of the total bony labyrinth volume; (3) the angle of the cochlea is less than 45° ; (4) the cochlea canal coils are less than $1\frac{1}{2}$ times; (5) the shape index of the cochlea canal is less than 0.90; (6) the shape index of the oval window is between 1.25 and 1.50; (7) the radius of curvature of the posterior semicircular canal is between 0.45 and 0.55; (8) the shape index of the posterior semicircular canal is less than 0.90; (9) the radius of curvature of the anterior semicircular canal is between 0.45 and 0.55; (10) the shape index of the anterior semicircular canals is between 0.90 and 1.10; (11) the radius of curvature of the lateral canal is between 0.45 and 0.55; (12) the shape index of the lateral semicircular canal is between 0.70 and 0.90; (13) the angle between the anterior and posterior semicircular canals is “obtuse”; (14) the angle between the anterior and lateral semicircular canals is “right”; (15) the angle between the posterior and lateral semicircular canals is “acute”; (16) the sagittal labyrinth index is between 10%

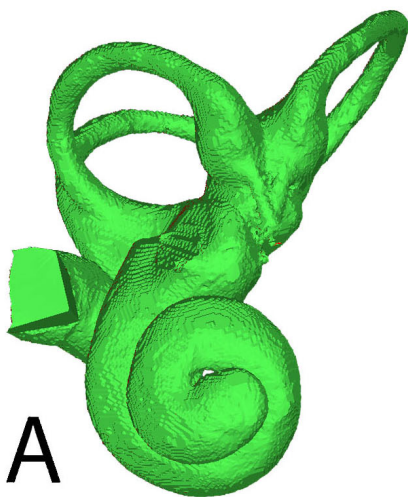


Figure 8 the bony labyrinth of the genus *Mesechinus* represented by A) *M. dauuricus* from NMB-9110

and 20%; (17) the ratio of the anterior relative to the posterior semicircular canal inner surface is between 1,05 and 2,05; (18) the ratio of the anterior relative to the lateral semicircular canal inner surface is between 0,95 and 1,05; (19) the ratio of the posterior relative to the lateral semicircular canal inner surface is between 0,95 and 1,05; (20) the ratio of the anterior relative to the posterior semicircular canal perimeter is greater than 1,05; (21) the ratio of the anterior relative to the lateral semicircular canal perimeter is greater than 1,05; (22) the ratio of the posterior relative to the lateral semicircular canal is between 0,95 and 1,05; (23) the ratio of the posterior semicircular length is between 15 and 30 times greater than the posterior semicircular length; (24) the ratio of the anterior semicircular length is between 15 and 30 times greater than the anterior semicircular length; (25) the ratio of the lateral semicircular length is up to 15 times greater than the lateral semicircular length.

Genus *Paraechinus* (Figure 9)

Description_ (1) percentage of common crus length is up to 40% of the total bony labyrinth length; (2) the percentage of the cochlea canal volume is between 40% and 50% of the total bony labyrinth volume; (3) the angle of the cochlea is less than 55° ; (4) the cochlea canal coils between $1\frac{1}{2}$ and 2 times; (5) the shape index of the cochlea canal is less than 1.10; (6) the shape index of the oval window is greater than 1.25; (7) the radius of curvature of the posterior semicircular canal is greater than 0.45; (8) the shape index of the posterior semicircular canal is less than 1.10; (9) the radius of curvature of the anterior semicircular canal is greater than 0.45; (10) the shape index of the anterior semicircular canals is between 0.70 and 1.10; (11) the radius of curvature of the lateral canal is greater than 0.45; (12) the shape index of the lateral semicircular canal has a great variety from smaller than 0.70 of *P. authiopicus* to greater than 0.90 for *P. micropus*; (13) the angle between

the anterior and posterior semicircular canal is “right”; (14) the angle between the anterior and lateral semicircular canal has a great variety of “acute” angles for *P. authiopicus* to “obtuse” angles for *P. hypomelas*; (15) the angle between the posterior and lateral semicircular canals varies from “acute” to “right”; (16) the sagittal labyrinth index is between 20% and 30%; (17) the ratio of the anterior relative to the posterior semicircular canal inner surface is greater than 1,05; (18) the ratio of the anterior relative to the lateral semicircular canal inner surface is lower than 1,05 for all members of *Paraechinus* with the exception of *P. hypomelas* which has a value greater than 2,05; (19) the ratio of the posterior relative to the lateral semicircular canal inner surface is lower than 0,95 for all species of the *Paraechinus* with the exception of *P. hypomelas* which has a value between 1,05 and 2,05; (20) the ratio of the anterior relative to the posterior semicircular canal perimeter is greater than 1,05; (21) the ratio of the anterior relative to the lateral 1,05; (22) the ratio of the posterior relative variety ranging from less than 0,95 for *P. authiopicus* to a value greater than 1,05 for *P. hypomelas*; (23) the ratio of the posterior semicircular length is up to 15 times greater than the posterior semicircular length; (24) the ratio of the anterior semicircular length is up to 30 times greater than the anterior semicircular length; (25) the ratio of the lateral semicircular length is up to 15 times greater than the lateral semicircular length.

Genus *Postpalerinaceus* (Figure 10)

Description_ (1) percentage of common crus length is between 30% and 50% of the total bony labyrinth length; (2) the percentage of the cochlea canal volume relative to the total bony labyrinth volume is unknown; (3) the angle of the cochlea is less than 45° ; (4) the cochlea canal coils less than $1\frac{1}{2}$ times; (5) the shape index of the cochlea canal is greater than 0.90; (6) the shape index of the oval window is

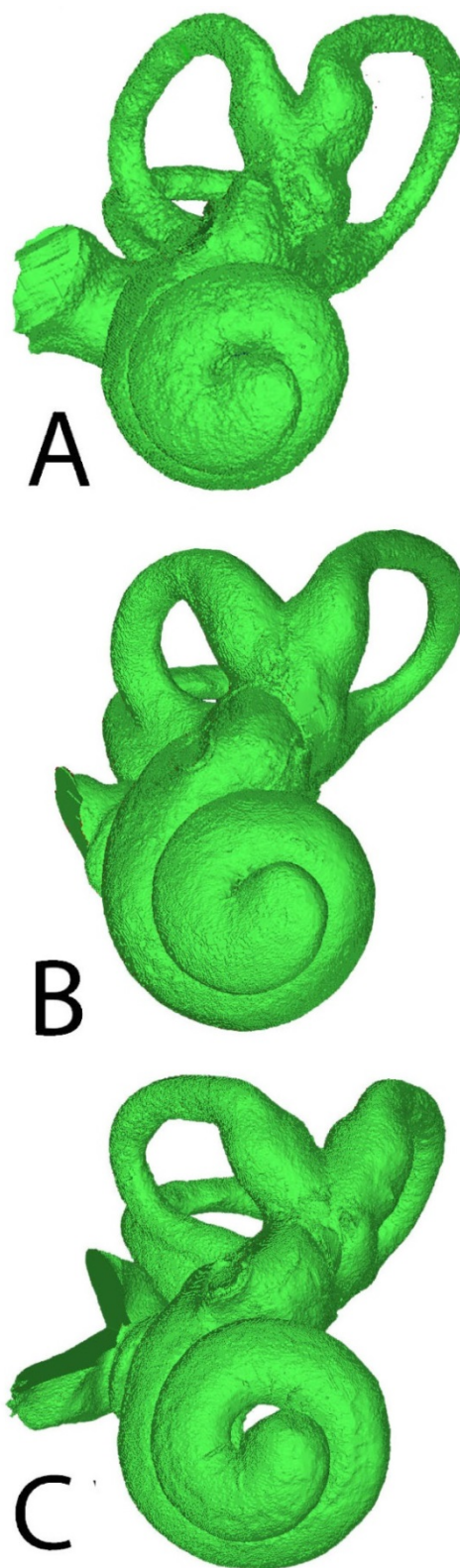


Figure 9 the bony labyrinth of the genus *Paraechinus* represented by A) *P. authiopicus* from NBC-ZMA.MAM.1765 B) *P. hypomelas* NMW-15242 and C) *P. micropus* NMW-15243

between 1.50 and 1.75; (7) the radius of curvature of the posterior semicircular canal is between 0.45 and 0.55; (8) the shape index of the posterior semicircular canal is between 0.90 and 1.10; (9) the radius of curvature of the anterior semicircular canal is less than 0.45; (10) the shape index of the anterior semicircular canals is a value between 0.90 and 1.10; (11) the radius of curvature of the lateral canal is between 0.45 and 0.55; (12) the shape index of the lateral semicircular canal is greater than 0.90; (13) the angle between the anterior and posterior semicircular canals is “acute”; (14) the angle between the anterior and lateral semicircular canals is “obtuse”; (15) the angle between the posterior and lateral semicircular canals is “acute”; (16) the sagittal labyrinth index is up to 20%; (17) the ratio of the anterior relative to the posterior semicircular canal inner surface is between 1,05 and 2,05; (18) the ratio of the anterior relative to the lateral semicircular canal inner surface is between 0,95 and 1,05; (19) the ratio of the posterior relative to the lateral semicircular canal inner surface is between 0,95 and 1,05; (20) the ratio of the anterior relative to the posterior semicircular canal perimeter is greater than 1,05; (21) the

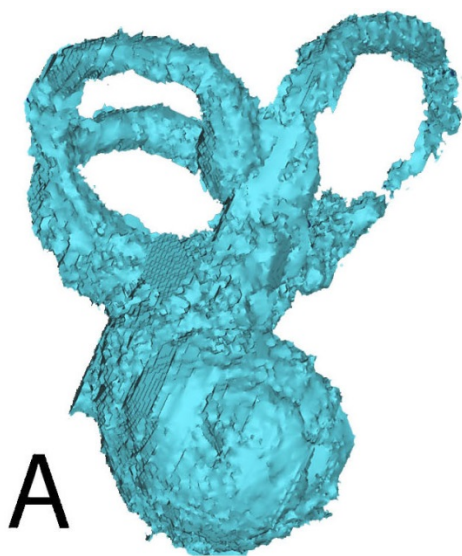


Figure 10 the bony labyrinth of the genus *Postpalerinaceous* represented by A) *Postpalerinaceous* sp. from MNCN-B-1051

ratio of the anterior relative to the lateral semicircular canal perimeter is greater than 1,05; (22) the ratio of the posterior relative to the lateral semicircular canal is between 0,95 and 1,05; (23) the ratio of the posterior semicircular length is between 15 and 30 times greater than the posterior semicircular length; (24) the ratio of the anterior semicircular length is unknown; (25) the ratio of the lateral semicircular length is up to 15 times greater than the lateral semicircular length.

Subgroup Galericinae

Genus *Echinosorex* (Figure 11)

Description (1) percentage of common crus length is between 30% and 40% of the total bony labyrinth length; (2) the percentage of the cochlea canal volume relative to the total bony labyrinth volume is greater than 60%; (3) the angle of the cochlea is less than 55°; (4) the cochlea canal coils is less than 2 times; (5) the shape index of the cochlea canal is less than 1.10; (6) the shape index of the oval window is between 1.25 and 1.75; (7) the radius of curvature of the posterior semicircular canal is between 0.45 and 0.55; (8) the shape index of the posterior semicircular canal is between 0.90 and 1.10; (9) the radius of curvature of the anterior semicircular canal is less than 0.45; (10) the shape index of the anterior semicircular canals is greater than 0.90; (11) the radius of curvature of the lateral canal is greater than 0.45; (12) the shape index of the lateral semicircular canal is between 0.70 and 0.90; (13) the angle between the anterior and posterior semicircular canal varies from “acute” to “right”; (14) the angle between the anterior and lateral semicircular canal varies between “acute” and “right”; (15) the angle between the posterior and lateral semicircular canals varies from “right” to “obtuse”; (16) the sagittal labyrinth index is up to 20%; (17) the ratio of the anterior relative to the posterior semicircular canal inner surface is between 1,05 and 2,05; (18) the ratio of the anterior relative to the

lateral semicircular canal inner surface is between 0,95 and 1,05; (19) the ratio of the posterior relative to the lateral semicircular canal inner surface is between 0,95 and 2,05; (20) the ratio of the anterior relative to the posterior semicircular canal perimeter is less than 0,95 for *E. rafflesi* but greater than 1,05 for *E. gymnurus*; (21) the ratio of the anterior relative to the lateral semicircular canal perimeter is less than 0,95 for *E. rafflesi* but greater than 1,05 for *E. gymnurus*; (22) the ratio of the posterior relative to the lateral semicircular canal is between 0,95 and 1,05; (23) the ratio of the posterior semicircular length is at least 15 times greater than the posterior semicircular length; (24) the ratio of the anterior semicircular length is at least 15 times greater than the lateral semicircular length; (25) the ratio of the lateral semicircular length is between 15 and 45 times greater than the lateral semicircular length.

Genus *Galerix* (Figure 12)

Description (1) percentage of common crus length is between 30% and 40% of the total bony labyrinth length; (2) the percentage of the cochlea canal volume relative to the total bony labyrinth volume is greater than 60%; (3) the angle of the cochlea is greater than 55° ; (4) the cochlea canal coils more than 2 times; (5) the shape index of the cochlea canal is between 0.90 and 1.10; (6) the shape index of the oval window is between 1.25 and 1.50; (7) the radius of curvature of the posterior semicircular canal is less than 0.45; (8) the shape index of the posterior semicircular canal is between 0.90 and 1.10; (9) the radius of curvature of the anterior semicircular canal is less than 0.45; (10) the shape index of the anterior semicircular canals is between 0.90 and 1.10; (11) the radius of curvature of the lateral canal is greater than 0.55; (12) the shape index of the lateral semicircular canal is between 0.70 and 0.90; (13) the angle between the anterior and posterior semicircular canal is “right”; (14) the angle between the anterior

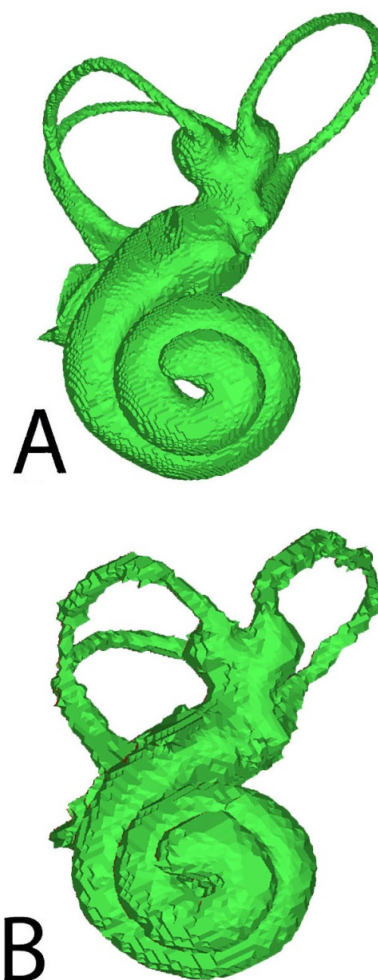


Figure 11 the bony labyrinth of the genus *Echinosorex* represented by A) *E. gymnurus* from NBC-RMNH.MAM.5061 and B) *E. rafflesi* from UMZC-E5111B

and lateral semicircular canal is “right”; (15) the angle between the posterior and lateral semicircular canals varies from lateral semicircular canals varies from “acute” to “right”; (16) the sagittal labyrinth index is between 20% and 30%;

(17) the ratio of the anterior relative to the posterior semicircular canal inner surface is between 1,05 and 2,05; (18) the ratio of the anterior relative to the lateral semicircular canal inner surface is between 0,95 and 1,05; (19) the ratio of the posterior relative to the lateral semicircular canal inner surface is between 0,95 and 1,05; (20) the ratio of the anterior relative to the posterior semicircular canal perimeter is greater than 1,05; (21) the

ratio of the anterior relative to the lateral semicircular canal perimeter is greater than 1,05; (22) the ratio of the posterior relative to the lateral semicircular canal is less than 0,95; (23) the ratio of the posterior semicircular length is between 15 and 30 times greater than the posterior semicircular length; (24) the ratio of the anterior semicircular length is between 15 and 30 times greater than the lateral semicircular length; (25) the ratio of the lateral semicircular length is between 15 and 30 times greater than the lateral semicircular length.

Genus *Hylomys* (Figure 13)

Description_ (1) percentage of common crus length is greater than 30% of the total bony labyrinth length; (2) the percentage of the cochlea canal volume relative to the total bony labyrinth volume is greater than 50%; (3) the angle of the cochlea has a great variety with fewer than 45° for *H. suillus dorsalis* but an cochlea angle greater than 55° for *H. s. peguensis*; (4) the cochlea canal coils are more than 2 times; (5) the shape index of the cochlea canal is lower than 1.10; (6) the shape index of the

oval window is greater than 1.25; (7) the radius of curvature of the posterior semicircular canal is less than 0.45; (8) the shape index of the posterior semicircular canal is greater than 0.90; (9) the radius of curvature of the anterior semicircular canal is less than 0.45; (10) the shape index of the anterior semicircular canals is between 0.70 and 1.10; (11) the radius of curvature of the lateral canal is between 0.45 and 0.55; (12) the shape index of the lateral semicircular canal is between 0.70 and 1.10; (13) the angle between the anterior and posterior semicircular canal varies between “acute” and “right”; (14) the angle between the anterior and lateral semicircular canal is “right”; (15) the angle between the posterior and lateral semicircular canals varies from “acute” to “right”; (16) the sagittal labyrinth index is greater than 20%; (17) the ratio of the anterior relative to the posterior semicircular canal inner surface is between 1,05 and 2,05; (18) the ratio of the anterior relative to the lateral semicircular canal inner surface is between 0,95 and 2,05; (19) the ratio of the posterior relative to the lateral semicircular canal inner surface is between 0,95 and 2,05; (20) the ratio of the anterior relative to the posterior semicircular canal perimeter is greater than 1,05; (21) the ratio of the anterior relative to the lateral semicircular canal perimeter is greater than 0,95; (22) the ratio of the posterior relative to the lateral semicircular canal shows a great variety ranging from small values below 0,95 from *H. suillus* to greater values of 1,05 or higher for *H. suillus peguensis*; (23) the ratio of the posterior semicircular length is between 15 and 45 times greater than the posterior semicircular length; (24) the ratio of the anterior semicircular length is at least 30 times greater than the lateral semicircular length; (25) the ratio of the lateral semicircular length is between 15 and 30 times greater than the lateral semicircular length.

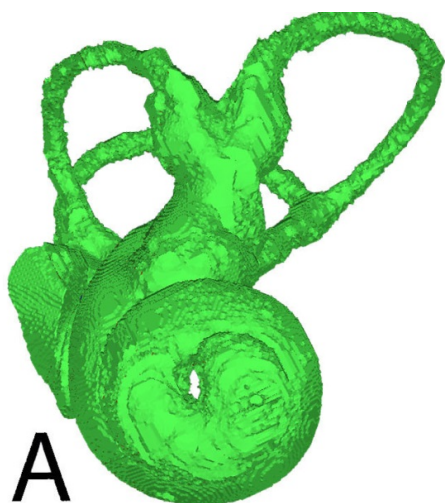


Figure 12 the bony labyrinth of the genus *Galerix* represented by A) *Galerix exilis* from NMW-XXX

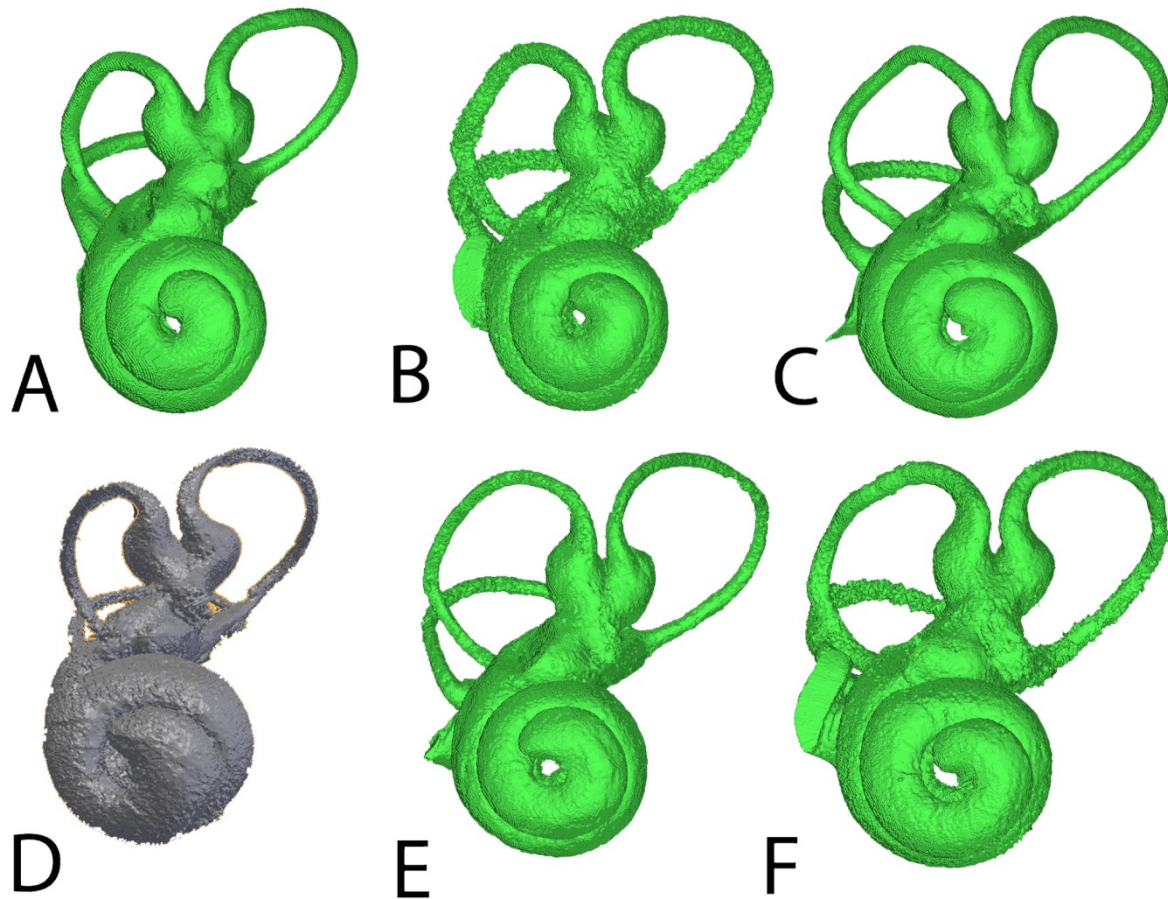


Figure 13 the bony labyrinth of the genera *Neotetracus* and *Hylomys* represented by A) *Neotetracus* sp. from NMB-XXX. B) *H. parvus* from NBC-RMNH.MAM.38335 C) *H. suillus* from NBC-ZMA.MAM.29225 D) *H. suillus dorsalis* from NBC-ZMA.Mam.29225 E) *H. s. maxi* from NBC.RMNH.MAM.38344 F) *H. s. suillus* from NBC.RMNH.Mam.12683

Genus *Neotetracus* (Figure 13)

Description (1) percentage of common crus length is between 30% and 40% of the total bony labyrinth length; (2) the percentage of the cochlea canal volume relative to the total bony labyrinth volume is between 50% and 60%; (3) the angle of the cochlea has a value less than 45° ; (4) the cochlea canal coils are more than 2 times; (5) the shape index of the cochlea canal is lower than 0.90; (6) the shape index of the oval window is between 1.25 and 1.50; (7) the radius of the curvature of the posterior semicircular canal is less than 0.45; (8) the shape index of the posterior semicircular canal is between 0.90 and 1.10; (9) the radius of curvature of the anterior semicircular canal is between 0.45 and 0.55; (10) the shape index of the anterior semicircular canals is greater than 1.10; (11) the radius of curvature of the

lateral canal is greater than 0.55; (12) the shape index of the lateral semicircular canal is between 0.70 and 0.90; (13) the angle between the anterior and posterior semicircular canals is “acute”; (14) the angle between the anterior and lateral semicircular canal is “right”; (15) the angle between the posterior and lateral semicircular canals is “right”; (16) the sagittal labyrinth index is between 20% and 30%; (17) the ratio of the anterior relative to the posterior semicircular canal inner surface is greater than 2,05; (18) the ratio of the anterior relative to the lateral semicircular canal inner surface is between 1,05 and 2,05; (19) the ratio of the posterior relative to the lateral semicircular canal inner surface is between 1,05 and 2,05; (20) the ratio of the anterior relative to the posterior semicircular canal perimeter is greater than 1,05; (21) the

ratio of the anterior relative to the lateral semicircular canal perimeter is greater than 1,05; (22) the ratio of the posterior relative to the lateral semicircular canal is between 0,95 and 1,05; (23) the ratio of the posterior semicircular length is 15 to 30 times greater than the posterior semicircular length; (24) the ratio of the anterior semicircular length is between 30 and 45; (25) the ratio of the lateral semicircular length is between 15 and 30 times greater than the lateral semicircular length.

Genus *Neurogymnurus* (Figure 14)

Description_ (1) percentage of common crus length is between 30% and 40% of the total bony labyrinth length; (2) the percentage of the cochlea canal volume relative to the total bony labyrinth volume is greater than 60%; (3) the angle of the cochlea has a value greater than 55° ; (4) the cochlea canal coils less than $1\frac{1}{2}$ times; (5) the shape index of the cochlea canal is between 0.90 and 1.10; (6) the shape index of the oval window is between 1.25 and 1.50; (7) the radius of curvature of the posterior semicircular canal is between 0.45 and 0.55; (8) the shape index of the posterior semicircular canal is between 0.70 and 0.90; (9) the radius of curvature of the anterior semicircular canal is between 0.45 and 0.55; (10) the shape index of the anterior semicircular canals is between 0.90 and 1.10; (11) the radius of curvature of the lateral canal is between 0.45 and 0.55; (12) the shape index of the lateral semicircular canal is greater than 1.10; (13) the angle between the anterior and posterior semicircular canal is “right”; (14) the angle between the anterior and lateral semicircular canal is “right”; (15) the angle between the posterior and lateral semicircular canals is “obtuse”; (16) the sagittal labyrinth index is between 10% and 20%; (17) the ratio of the anterior relative to the posterior semicircular canal inner surface is between 1,05 and 2,05; (18) the ratio of the anterior relative to the lateral semicircular canal inner surface is

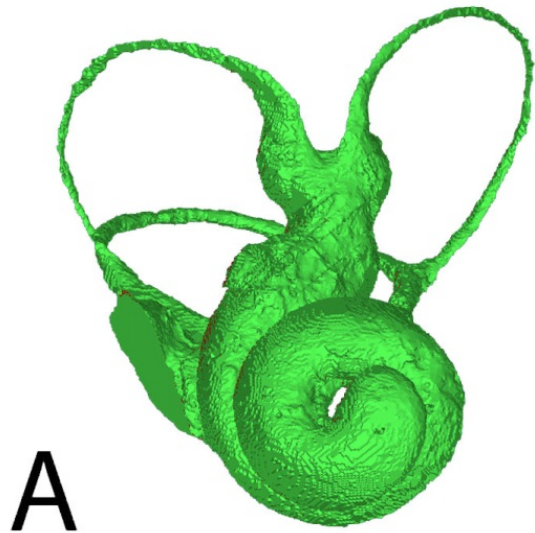


Figure 14 the bony labyrinth of the genus *Neurogymnurus* represented by A) *Neurogymnurus* sp. from NMB-QH391

between 0,95 and 1,05; (19) the ratio of the posterior relative to the lateral semicircular canal inner surface is between 1,05 and 2,05; (20) the ratio of the anterior relative to the posterior semicircular canal perimeter is greater than 1,05; (21) the ratio of the anterior relative to the lateral semicircular canal perimeter is greater than 1,05; (22) the ratio of the posterior relative to the lateral semicircular canal is between 0,95 and 1,05; (23) the ratio of the posterior semicircular length is more than 45 times than the posterior semicircular length; (24) the ratio of the anterior semicircular length is between 30 and 45; (25) the ratio of the lateral semicircular length is more than 45 times greater than the lateral semicircular length.

Parasorex (Figure 15)

Description_ (1) percentage of common crus length is between 40% and 50% of the total bony labyrinth length; (2) the percentage of the cochlea canal volume relative to the total bony labyrinth volume is unknown; (3) the angle of the cochlea has a value greater than 55° ; (4) the cochlea canal coils are between $1\frac{1}{2}$ and 2 times; (5) the shape index of the cochlea canal is between 0.90 and 1.10; (6) the shape index of the oval window is less

than 1.25; (7) the radius of curvature of the posterior semicircular canal is between 0.45 and 0.55; (8) the shape index of the posterior semicircular canal is between 0.90 and 1.10; (9) the radius of curvature of the anterior semicircular canal is greater than 0.55; (10) the shape index of the anterior semicircular canals is between 0.90 and 1.10; (11) the radius of curvature of the lateral canal is greater than 0.55; (12) the shape index of the lateral semicircular canal is between 0.90 and 1.10; (13) the angle between the anterior and posterior semicircular canals is “acute”; (14) the angle between the anterior and lateral semicircular canals is “obtuse”; (15) the angle between the posterior and lateral semicircular canals is “right”; (16) the sagittal labyrinth index is between 20% and 30%; (17) the ratio of the anterior relative to the posterior semicircular canal inner surface is between 1,05 and 2,05; (18) the ratio of the anterior relative to the lateral semicircular canal inner surface is between 0,95 and 1,05; (19) the ratio of the posterior relative to the lateral semicircular canal inner surface is less than 0,95; (20) the ratio of the anterior lateral semicircular canal inner surface is less than 0,95; (20) the ratio of the anterior relative to the posterior semicircular canal perimeter is greater than 1,05; (21) the ratio of the anterior relative to the lateral semicircular canal perimeter is greater than ratio of the anterior relative to the lateral semicircular canal perimeter is greater than 1,05; (22) the ratio of the posterior relative to the lateral semicircular canal is between 0,95 and 1,05; (23) the ratio of the posterior semicircular length is between 15 and 30 times than the posterior semicircular length; (24) the ratio of the anterior semicircular length is between 15 and 30; (25) the ratio of the lateral semicircular length is less than 15 times greater than the lateral semicircular length.

Outgroup

Genus *Solenodon cubanus* (Figure 16)

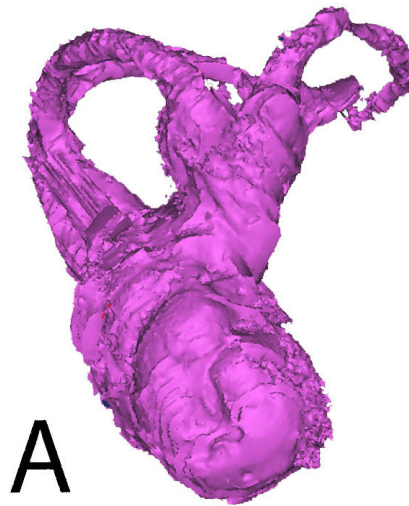


Figure 15 the bony labyrinth of the genus *Parasorex* representat by A) *Parasorex* sp. MNCN-BAT-1-2002-C7-12

Description_ (1) percentage of common crus length is less than 30% of the total bony labyrinth length; (2) the percentage of the cochlea canal volume relative to the total bony labyrinth volume is between 50% and 60%; (3) the angle of the cochlea has a value less than 45° ; (4) the cochlea canal coils more than 2 times; (5) the shape index of the cochlea canal is less than 0.90; (6) the shape index of the oval window is between 1.50 and 1.75; (7) the radius of curvature of the posterior semicircular canal is between 0.45 and 0.55; (8) the shape index of the posterior semicircular canal is between 0.70 and 0.90; (9) the radius of curvature of the anterior semicircular canal is between 0.45 and 0.55; (10) the shape index of the anterior semicircular canals is between 0.90 and 1.10; (11) the radius of curvature of the lateral canal is between 0.45 and 0.55; (12) the shape index of the lateral semicircular canal is greater than 1.10; (13) the angle between the anterior and posterior semicircular canal is “right”; (14) the angle between the anterior and lateral semicircular canal is “right”; (15) the angle between the posterior and lateral semicircular canals is “obtuse”; (16) the sagittal labyrinth index is between 20% and 30%; (17) the ratio of the anterior relative to the posterior semicircular canal inner surface is between 1,05 and 2,05;

(18) the ratio of the anterior relative to the lateral semicircular canal inner surface is between 0,95 and 1,05; (19) the ratio of the posterior relative to the lateral semicircular canal inner surface is between 1,05 and 2,05; (20) the ratio of the anterior relative to the posterior semicircular canal perimeter is greater than 1,05; (21) the ratio of the anterior relative to the lateral semicircular canal perimeter is greater than 1,05; (22) the ratio of the posterior relative to the lateral semicircular canal is greater than 1,05; (23) the ratio of the posterior semicircular length is between 15 and 30 times than the posterior semicircular length; (24) the ratio of the anterior semicircular length is between 15 and 30; (25) the ratio of the lateral semicircular length is less than 15 times greater than the lateral semicircular length.

Genus *Setifer setosus* (Figure 17)

Description_ (1) percentage of common crus length is less than 30% of the total bony labyrinth length; (2) the percentage of the cochlea canal volume relative to the total bony labyrinth volume is between the total bony labyrinth volume is between 40% and 50%; (3) the angle of the cochlea has a value less than 45° ; (4) the cochlea canal coils are between $1\frac{1}{2}$ and 2 times; (5) the shape index of the cochlea canal is



Figure 16 the bony labyrinth of the genus *Solenodon* represented by A) *Solenodon cubanus* from UMZC-E5418B



Figure 17 the bony labyrinth of the genus *Setifer* represented by A) *Setifer setosus* from UMZC E5450B

the total bony labyrinth volume is between 40% and 50%; (3) the angle of the cochlea has a value less than 45° ; (4) the cochlea canal coils are between $1\frac{1}{2}$ and 2 times; (5) the shape index of the cochlea canal is less than 0.90; (6) the shape index of the oval window is between 1.25 and 1.50; (7) the radius of curvature of the posterior semicircular canal is between 0.45 and 0.55; (8) the shape index of the posterior semicircular canal is between 0.70 and 0.90; (9) the radius of curvature of the anterior semicircular canal is between 0.45 and 0.55; (10) the shape index of the anterior semicircular canals is greater than 1.10; (11) the radius of curvature of the lateral canal is between 0.45 and 0.55; (12) the shape index of the lateral semicircular canal is greater than 1.10; (13) the angle between the anterior and posterior semicircular canals is “acute”; (14) the angle between the anterior and lateral semicircular canals is “acute”; (15) the angle between the posterior and lateral semicircular canals is “right”; (16) the sagittal labyrinth index is greater than 30%; (17) the ratio of the anterior relative to the posterior semicircular canal inner surface is between 1,05 and 2,05; (18) the ratio of the anterior relative to the lateral semicircular canal inner surface is between

0,95 and 1,05; (19) the ratio of the posterior relative to the lateral semicircular canal inner surface is between 1,05 and 2,05; (20) the ratio of the anterior relative to the posterior semicircular canal perimeter is between 0,95 and 1,05; (21) the ratio of the anterior relative to the lateral semicircular canal perimeter is greater than 1,05; (22) the ratio of the posterior relative to the lateral semicircular canal is greater than 1,05; (23) the ratio of the posterior semicircular length is between 30 and 45 times the posterior semicircular length; (24) the ratio of the anterior semicircular length is between 15 and 30 times the anterior semicircular length; (25) the ratio of the lateral semicircular length is between 15 and 30 times the length of the lateral semicircular.

Phylogenetic trees

In total five different phylogenetic trees were made for the family Erinaceidae. Two trees were based on the 25 characters of the bony labyrinth, once with only extant species (Figure 18) and once with both extinct and extant species (Figure 19). The next tree was founded on the combination of the 3177 characters of the DNA material (12S, CytB and NADH) and the 197 characters of the joined datasets of Gould 1995 and 2001, with both extant and extinct species included (Figure 20). The last two trees were constructed by uniting all datasets, the bony labyrinth, the DNA and morphological material, creating a 3399 characteristics dataset. One tree was based on extant species only (Figure 21), while the other tree included both extinct and extant species (Figure 22).

The heuristic search was conducted under the majority rule consensus with a replication rate of 1000. The numbers above the nodes represents the percentage the group is found to which the node is the base. With the majority rule consensus, only groups found at least 50% of the replication rate are shown. However, a group occurring 51% of the time is only slightly more reliable than a group

occurring 49% of the time. Therefore, when judging the likelihood of a group, only values from 70% up were considered probable (Braun and Kimball, 2002; Zander, 2004)

Discussion bony labyrinth characters

The bony labyrinth characters used for parsimony tree

Of the 25 characters of the bony labyrinth, a total of 24 were parsimony informative. They were compatible only in some trees, whereas the parsimony uninformative characteristic, the ratio of the perimeter between the anterior semicircular canal relative and the lateral semicircular canal (21), was compatible for all trees, giving no further information in the search for most parsimony tree

The bony labyrinth characters used for determination

Of the 25 characters of the bony labyrinth, 5 showed great variation in morphological condition on the following characters; the shape index of the oval window (6), the angle between the anterior and posterior semicircular canal (13), the angle between the posterior and lateral semicircular canal (15), the ratio of the perimeter of the anterior semicircular canal relative to the posterior semicircular canal (20) and the ratio of the perimeter of the posterior semicircular canal relative to the lateral semicircular canal (22). When the two subgroups Erinaceinae and Galericinae are separated, the different character states of these five characters are diffused between both subgroups. Although this does not make them less important in the selection on genus level, for the distinction between Erinaceinae and Galericinae they cannot be used. The nine different characters that do help discriminate extant Erinaceinae from extant Galericinae are the cochlea volume relative to the total volume of the bony labyrinth (2), the number of coils in the cochlea canal (4), the radius of curvature of the posterior semicircular canal (7), the shape index of the posterior semicircular

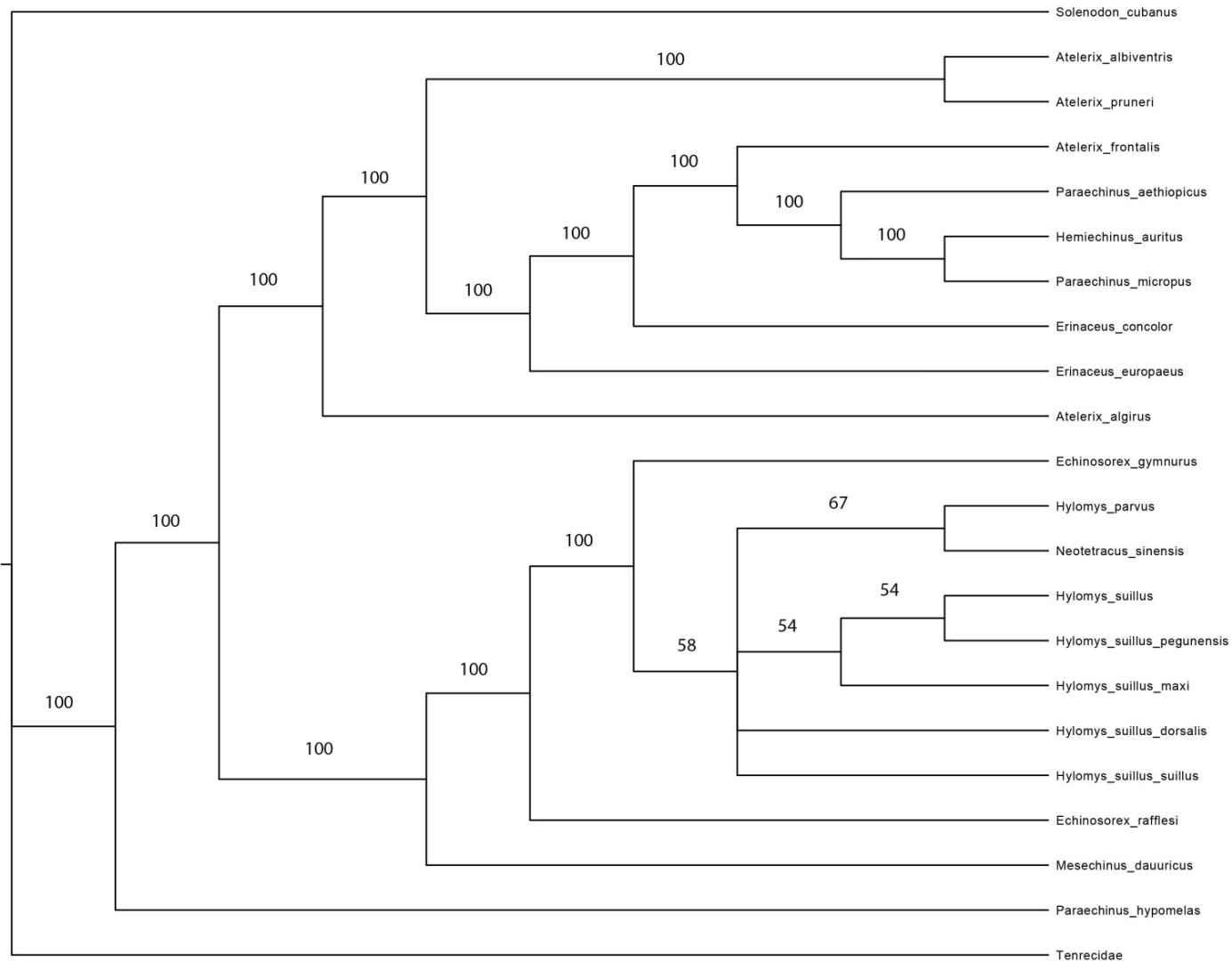


Figure 18 Results of the heuristic search with majority rule consensus analysis (nreps=1000 addseq=random) based on 25 bony labyrinth characters. Only extant Erinaceidae (19 in total) were included together with 2 outgroups. The number above the nodes represents the percentage of the clade found, with a minimum of 50%.

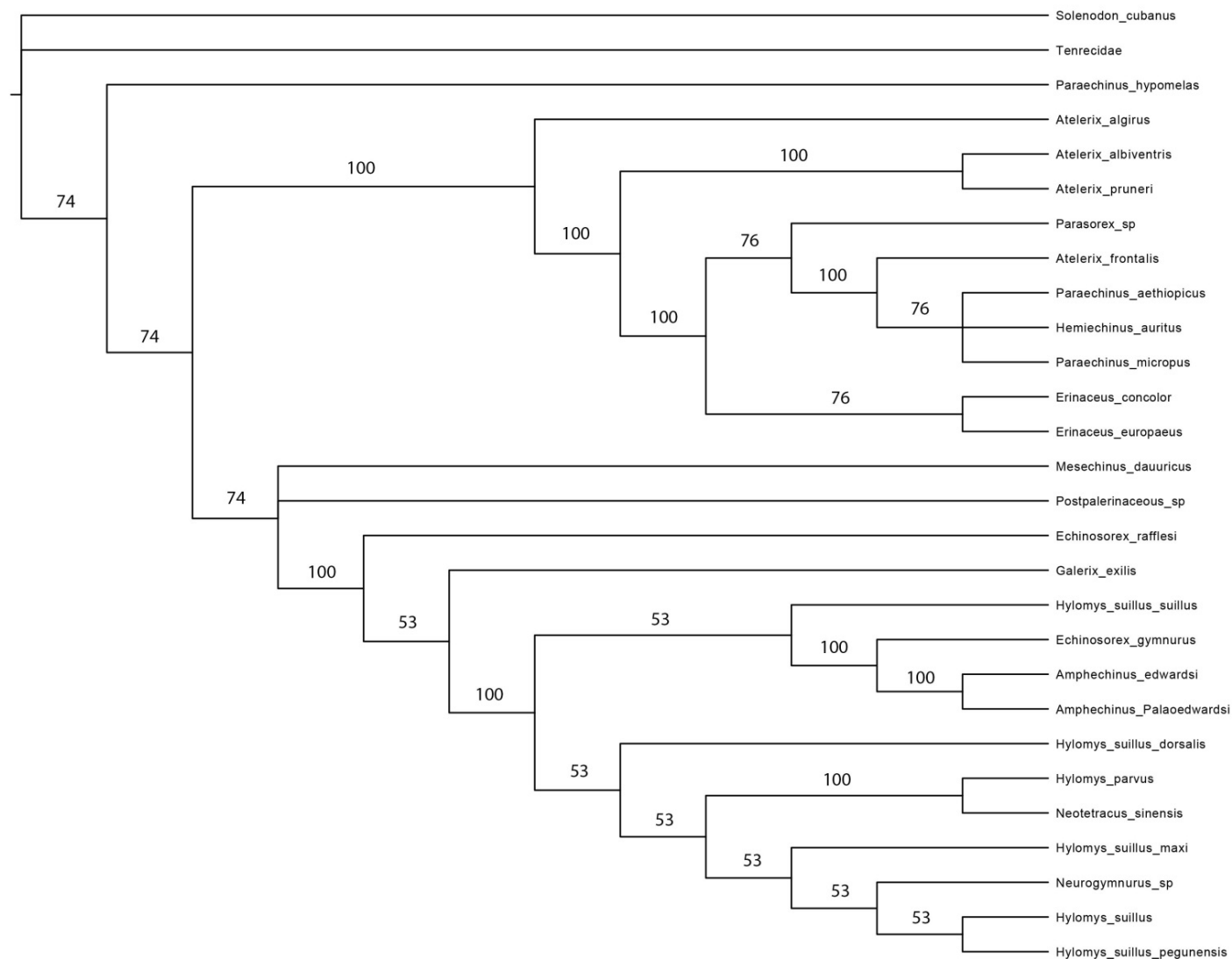


Figure 19 Results of the heuristic search with majority rule consensus analysis (nreps=1000 addseq=random) based on 25 bony labyrinth characters. From the family Erinaceidae 19 extant and 7 extinct species were included in this tree, together with 2 outgroups. The number above the nodes represents the percentage of the clade found, with a minimum of 50%.

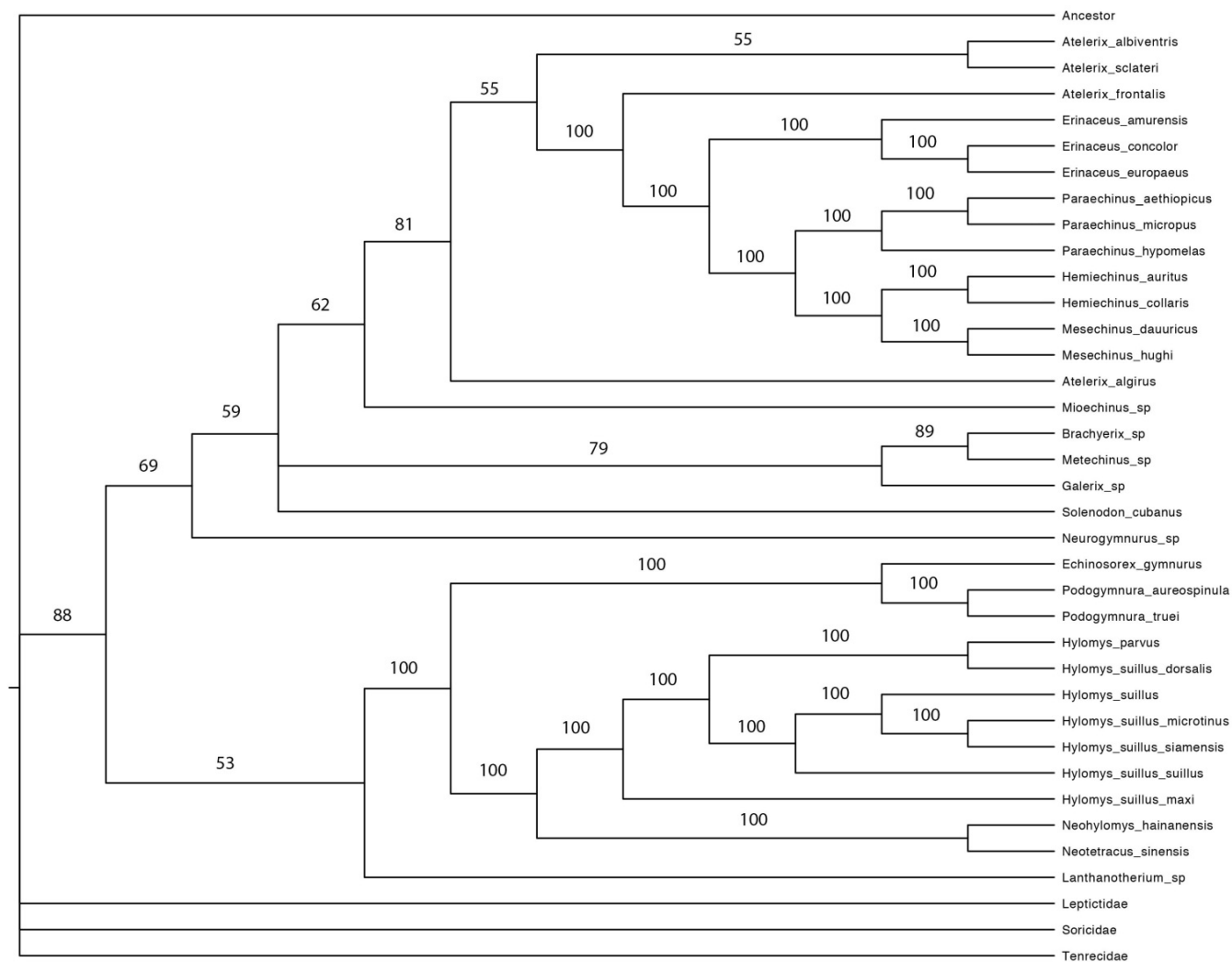


Figure 20 Results of the heuristic search with majority rule consensus analysis (nreps=1000 addseq=random) based on a combination of 3177 DNA material characters (12S, CytB and NADH) and the combination of the 197 morphological characters from Gould 1995 and 2001. From the family Erinaceidae 27 extant and 5 extinct species were included in this tree, together with 5 outgroups. The number above the nodes represents the percentage of the clade found, with a minimum of 50%.

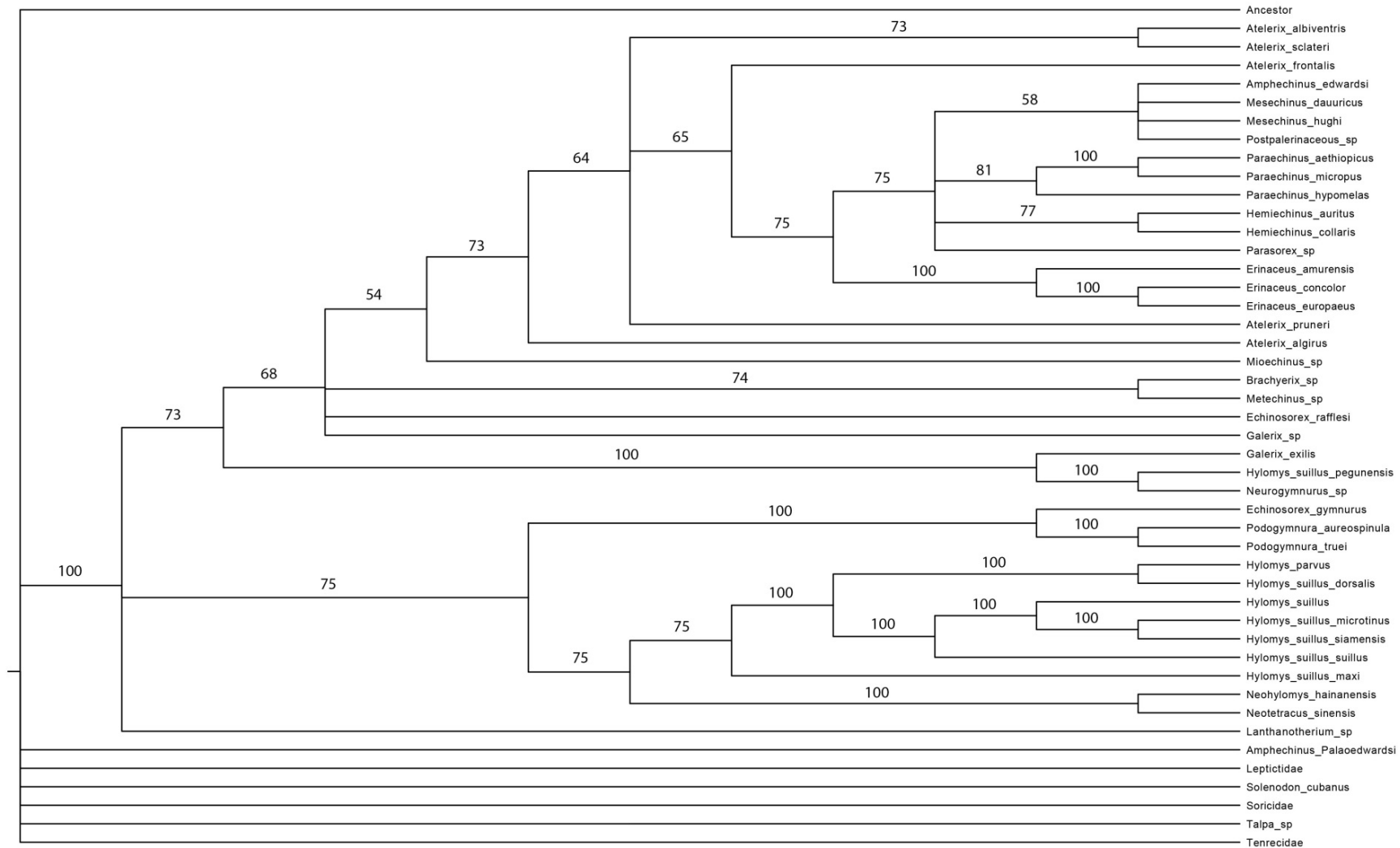


Figure 22 Results of the heuristic search with majority rule consensus analysis (nreps=1000 addseq=random) based on a combination of 3177 DNA material characters (12S, CytB and NADH), the combination of the 197 morphological characters from Gould (1995, 2001) and 25 bony labyrinth characters. From the family Erinaceidae 29 extant and 11 extinct species were included in this tree, together with 6 outgroups. The number above the nodes represents the percentage of the clade found, with a minimum of 50%.

canal (8), the shape index of the anterior semicircular canal (10), the sagittal labyrinth index (16), the ratio of the length relative to the diameter of the posterior semicircular canal (23), the ratio of the length relative to the diameter of the anterior semicircular canal (24) and the ratio of the length relative to the diameter of the lateral semicircular canal (25). With this description only the extant species (Figures 4, 5, 6, 7, 8, 8, 11 and 13) were used, as the data from the fossils were either incomplete (e.g. *Parasorex*, Figure 15) or too counter-intuitive (e.g. *Amphichinus*, Figure 4).

Exclusive character states (Appendix table 4) for extant Erinaceinae are; (2) a cochlea canal volume less than 50% compared to the total bony labyrinth; (4) a coiling less than 1 ½ turns of the cochlea; (7) the radius of the curvature of the posterior semicircular circle is greater than 0.55; (8) the radius of the curvature of the anterior semicircular canal is less than 0.70; (10) the shape index of the anterior semicircular canal is less than 0.70; (23) the length of the posterior semicircular canal is less than 15 times the diameter; (24) the length of the anterior semicircular canal is less than 15 times the diameter; (25) the length of the lateral semicircular canal is less than 15 times the diameter. Exclusive character states for extant Galericinae are; (2) a cochlea canal volume greater than 60% compare to the total bony labyrinth; (4) a cochlea coiling more than 2 turns; (8) the radius of the curvature of the anterior semicircular canal is greater than 0.90; (16) a sagittal labyrinth index lower than 10 or greater than 30; (23) the length of the posterior semicircular canal is greater than 30 times the diameter; (24) the length of the anterior semicircular canal is greater than 30 times the diameter; (25) the length of the lateral semicircular canal is greater than 15 times the diameter. This does not mean that these are the only characteristic states found within Erinaceinae or Galericinae, but it signifies that these are

the characteristic states that are not shared between them.

Discussion phylogenetic trees

Most parsimony tree based on molecular DNA and morphology

The topology of the phylogenetic tree based on the combination of the matrices from Gould (1995, 2001) and the aligned DNA sequences CytB, NADH and 12S (Figure 20) shows a clear division between Erinaceinae and Galericinae. Most genera form a neat monophyletic group (e.g., *Erinaceus*, *Hemiechinus*, *Hylomys*, *Paraechinus*, *Podogymnura* and *Mesechinus*) but there are still some species of which the position is counter-intuitive to say the least. To start with the outgroup *Solenodon cubanus*, which is not placed with the other outgroup species but instead is placed in an intermediate position between Galericinae and Erinaceinae, even though it is clear that *S. cubanus* is not a member of the Erinaceidae but of the Solenodontidae (Morgan and Ottenwalder, 1993; Roca *et al.*, 2004). It could be that the fusion of the two datasets (DNA and morphology of Gould) did not succeed because one set placed *S. cubanus* more towards the Erinaceinae, while the other dataset claimed a relationship closer to Galericinae, resulting in a place in the middle of the phylogenetic tree. The extinct groups *Brachyerix*, *Metechinus* and *Galerix* form their own cluster, basal to the extant Erinaceinae. The extinct groups are therefore not integrated into the rest of the tree as would have otherwise been expected. *Mioechinus* is the direct sister group of the other (extant) Erinaceinae. The positioning of the genus *Lantanothereum*, at the basal branch of the Galericinae, seems legitimate since the genus died out in the mid Miocene (Table 1). The position could well indicate a more primitive morphology relative to the extant genera used in the matrix. One might expect the extinct genus *Neurogymnurus* to join *Lantanothereum* at the basal branch, since *Neurogymnurus* is considered to be the most primitive of the Erinaceidae (Butler

1948; Leche, 1902, 1920), as well as being the oldest Erinaceidae found in the fossil record. However *Neurogymnurus* is positioned as the sister group of the Erinaceinae and *Solenodon cubanus* and therefore forms a paraphyletic group with respect to Galericinae. Although *Neurogymnurus* shares characters with both *Echinosorex* and *Galerix* (e.g., enlarged canines and maxilla above the orbit), in other aspects, such as the mastoid region, *Neurogymnurus* resembles *Brachyerix* and *Metechinus* (Butler, 1948; Mathew and Mook, 1933; Meade, 1941). When comparing these observations with the position *Neurogymnurus* takes in the various phylogenetic trees (Figure 19, 20 and 22) he is placed right between Erinaceinae and Galericinae, but more importantly as a sistergroup of other extinct Erinaceidae, suggesting a closer similarity between extinct genera in general than towards their extant subgroup members. Furthermore, the genus *Hylomys* forms a monophyletic group but instead of having a basal splitting between *Hylomys parvus* and the remaining *Hylomys suillus* sp. the first side branch is made by *Hylomys suillus maxi* and *Hylomys parvus* has the sistergroup *Hylomys suillus dorsalis*.

Most parsimony tree based on the bony labyrinth

The 25 characteristic datasets of the bony labyrinth from the 26 species of Erinaceidae and two outgroups were used to make a phylogenetic tree solely based on the inner ear with the exclusion of fossils (Figure 18). To investigate the effect fossils have on the position of extant species in the phylogenetic tree, the exact same database was used to make a tree, with the addition of fossil data (Figure 19).

When no fossils are used (Figure 18), the division between Erinaceinae and Galericinae is roughly intact. The members of the genera *Atelerix*, *Echinosorex*, *Erinaceus* and *Hylomys* are all still clustered together and placed within their subgroup of

Erinaceinae or Galericinae respectively. The only exception being the species *Mesechinus dauuricus* and *Paraechinus hypomelas*. The Erinaceinae *Mesechinus dauuricus* is placed in a way that indicates a stronger relationship to the Galericinae clade and *Paraechinus hypomelas* is positioned basally to the division of Erinaceinae and Galericinae. Furthermore, there is a paraphyletic clade formed by the unresolved group of *Hylomys* together with *Neotetracus sinensis*. Although the strong resemblance in morphology has been repeatedly confirmed (Butler, 1948; Corbet 1988, whether or not they are actually congener has been both suggested (van Valen, 1967; Nowak and Paradiso, 1983) and rejected (Heaney and Morgan, 1982). Given the strong similarities within the genus *Hylomys*, the expectations of a clear group based on a mere 25 bony labyrinth characteristics might have been too demanding. This is made clear by the few branches within the *Hylomys* and *Neotetracus* group. The values above the branches are so low (e.g., 54, 58 and 67), that they can be considered non-existing, creating one unclear polytomy after the division with *Echinosorex gymnurus*.

When fossils are included the clear division between Erinaceinae and Galericinae is slightly weakened, mainly because of the positioning of extinct Erinaceidae placed in the opposite subgroup (e.g., *Parasorex* and *Amphechinus*). For starters the genus *Parasorex* was placed as a sistergroup of the Erinaceinae genera *Atelerix*, *Paraechinus* and *Hemiechinus*, while *Parasorex* in general is associated with *Galerix*, (Viret, 1938; Baudelot, 1972; Ziegler and Daxner-Höck, 2005), *Deinogalerix* (van den Hoek Ostende, 2001) and *Schizogalerix* (Viller et al., 2013), all genera within the subgroup of Galericinae. When comparing the character states for *Parasorex* sp. to *Hemiechinus auritus* shares 16 out of 25 character states, meanwhile *Galerix exilis* shares only 12 out of 25 character states, none of which are exclusive for the two (Appendix table 4).

All character states that are the same for *Parasorex* sp. and *Galerix exilis* are shared with at least one of the genera placed as a sistergroup for *Parasorex* sp. (Figure 19 and 22). Based on the measurements used to create the matrix, the placement of *Parasorex* sp. within the Erinaceinae clade seems justified. However this conclusion is drawn under the impression that the measurements are done on a bony labyrinth in good condition and sadly this is not the case. When examining *Parasorex* sp. (Figure 15), describing the state of the bony labyrinth slightly damages would be an understatement. When conducting a reconstruction, adjustments can be made for gaps or chips in the object, but such a reconstruction would, at least partly, be based on speculation instead of on solid measurements. This type of reconstruction has been used in a variety of disciplines, for both geological (Farke et al., 2013; Prieto-Márquez and Wagner, 2013) and anthropological (Abate et al., 2003) purposes and it has been proven to be a valuable tool in perfecting the reconstruction of objects who due to damage would have remained incomplete, as is often the case with fossils. Nonetheless, for the sake of time no attempted were made to improve the condition of *Parasorex* sp. Looking back, this decision might have been made too hasty and a redo of the bony labyrinth of *Parasorex* sp. would most certainly result in changes of the character states and could influence the position of *Parasorex* sp. in the phylogenetic tree.

On the other hand, the scans of the genus *Amphechinus*, previously described as a member of the Erinaceinae (Butler, 1956, Gawne, 1968; Sulimski, 1970; Ziegler 2005), are both very clear, limiting the possibility that wrong measurements were the cause of the position that *Amphechinus* holds in the tree (Figure 19). In this tree *Amphechinus edwardsi* and *A. palaoedwardsi* are placed into the same cluster with *Echinosorex gymnurus* as their sistergroup, right in the middle of all the

Galericinae members. Furthermore, when comparing the morphology of bony labyrinth with *Echinosorex gymnurus* out of the 25 characteristic states 22 are shared, creating a huge likeliness. The only traits that differ are regarding the shape and size of the cochlea canal, which coils just under two turns for *Amphechinus*, while the cochlea canal coils more than two times for *Echinosorex*. As a result, the percentage of cochlea volume compare to the entire bony labyrinth is greater for *Echinosorex* than for *Amphechinus*, but apart from these minor details the bony labyrinth are almost identical. However, the bony labyrinth is only a small character set, and based on numerous dental characteristics (e.g., enlargement of I2 and perforation of the palate) the position of *Amphechinus* in the midst of Erinaceidae seems stable. Nonetheless, it would be curious to see if the extinct Erinaceinae genera *Brachyerix* and *Metechinus*, who presumably did evolve from *Amphechinus*-like ancestors (McKenna and Holton, 1967) followed in their footsteps and had bony labyrinth similar to extant Galericinae with high coils of the cochlea canal and thin semicircular canals. Or alternatively, did the genera *Brachyerix* and *Metechinus* became more like extant Erinaceinae, with few turns in the cochlea canal and thick semicircular canals.

Furthermore, the paraphyletic formed by the unresolved group of *Hylomys* together with *Neotetracus sinensis* is still present when fossils are added to the database (Figure 19). As stated earlier when reviewing the phylogenetic tree based on the bony labyrinth without fossils (Figure 18), the high similarity between the members of *Hylomys* resulted in a polytomy, but now with the extinct genus *Neurogymnurus* included. Even though it looks like this resolved when fossils are added, when comparing the values above the branches (e.g., 53) that they can be considered non-existent leaving the *Hylomys* group tangled. The only exception being the group *Hylomys parvus* and *Neotetracus sinensis*.

Their relationship has strengthened compare to the situation with no fossils.

Parsimony tree based on the combination of molecular DNA, morphology and the bony labyrinth

The combined analyses containing all the data, 3399 characters of 52 Erinaceidae species and five outgroups was run twice, once with only extant species (Figure 21) and once with extinct species included (Figure 22).

When fossils are included, the tree shows more consistency with the tree based on the combination of the morphological characters from Gould (1995, 2001) and the molecular DNA (Figure 21). The arrangement of branches in the Erinaceinae clade for *Erinaceus*, *Hemiechinus*, *Paraechinus*, and *Mesechinus* are identical in both trees. The only difference is the addition of particular species within the genus *Atelerix* resulting in the formation of *Atelerix* as a monophyletic group. More differences are evident in the Galericinae clade. To start, the base of the Galericinae clade is not fully resolved, forming a four-way polytomy of the monophyletic group *Podogymnura*, *Echinosorex gymnurus*, *Echinosorex rafflesi* and one large remaining clade comprising of *Hylomys*, *Neohylomys* and *Neotetracus*. The latter two do not have a clear relationship since they form a polytomy with the *Hylomys* clade, giving another paraphyletic group.

When fossils are included in the database, the topology of genera such as *Atelerix*, which formed monophyletic clades without fossils, break up and become scattered. The only monophyletic group remaining in the Erinaceinae clade is *Erinaceus*, while all other genera are involved in polytomous nodes, giving an unclear ancestral pattern. The genus *Amphechinus* is completely divided with *A. edwardsi* recovered within the Erinaceidae, while *A. palaeoedwardsi* is located among the outgroups at the base of

the tree. In contrast, as tangled as the Erinaceinae clade becomes when fossils are included, the Galericinae clade becomes more clearly resolved. All the *Hylomys* are recovered in one group, with the exception of *H. suillus pegunensis*. The genus *Podogymnura* is a monophyletic group, and only the genus *Echinosorex* has members widely spaced within the tree. *Echinosorex rafflesi* is separated from the other Galericinae and placed as a side branch of the extinct Erinaceinae *Galerix*, *Brachyerix*, *Metechinus*, and *Mioechinus*. Although this could suggest that *Echinosorex rafflesi* possesses Erinaceinae treads, based on position of *Echinosorex gymnurus*, which is always positioned in the Galericinae clade (Figure 18 until 22), this seems unlikely. Although it is not impossible, it seems improbable that two well defined and documented species (Frost, 1991; Gould, 1995) from the same genus to be separated in a phylogenetic tree. Instead the source the placement for *E. rafflesi* can be found in the quality of the scan used to measure the characteristics of the bony labyrinth. The setting for the scanning of *E. rafflesi* was different from most other scans because of the voxelsize (thickness of the slices, which when put together create a 3D image). The scan generously offered by the University Museum of Zoology Cambridge (Figure 11.B, Appendix table 1) was scanned with a very high voxelsize. As a consequence, the details found in other scans (e.g., the *Echinosorex gymnurus* scan from Naturalis Biodiversity Center, Figure 11.A, Appendix table 1) are missing in a 3D reconstruction. Any measurement taken from such a pixelated 3D reconstruction will deviate ever so slightly from the original shape of the bony labyrinth. Even though the differences are minimal, it could be enough to influence the position of *E. rafflesi* in the phylogenetic tree.

General pattern

All the phylogenetic trees (Figures 18 until 22) generally show the same monophyletic

clades for the genera *Erinaceus*, *Mesechinus*, *Paraechinus*, and *Hemiechinus*. The most basal clade is *Erinaceus*, followed by progressively more nested clades of *Paraechinus* and the sister groups *Hemiechinus* and *Mesechinus*. This pattern is consistent with the earlier trees found in He et al. (2012) based on the DNA sequences CytB, NADH and 12S (Figure 6, page 7) and the combined-gene tree (Figure 7, page 8).

A similar pattern can be found within the Galericinae clade, where *Echinosorex* and *Podogymnura* are always sister clades and are always more basal than the *Neotetracus*, *Neohylomys* and *Hylomys* clades. Although the underlying relations of these latter three groups show more variation, in general the *Neotetracus* and *Neohylomys* are resolved as sister groups more basal to the clade of *Hylomys* as in contrast to the combined-gene tree (Figure 7, page 8) of He et al. (2012), where *Neohylomys* is most basal, with *Neotetracus* and *Hylomys* progressively nested in the clade.

Influence of Fossils

When the extinct Erinaceidae are added to the database their influence depends on the amount of other data sources used to create the tree (e.g., DNA, morphology or the characteristic of the bony labyrinth). The species with two or more out of the three categories are more likely to cluster together, as are the species based on only one type of data. So does the position of fossils (e.g. *Postpalerinaceus* or *Amphechinus*) vary considerably in their place in the tree when molecular or morphological characters other than the bony labyrinth are included. An explanation for this behaviour could be the relatively low number of morphological and molecular characters in the dataset for fossils. Since most of them only contribute to the database in the form of the 25 characters from the bony labyrinth, this might not weight equally as the 3374

characters from the remaining databases. A solution to this problem might be weighting the data, in order to improve the influence of the bony labyrinth characters.

A way to avoid weighting might be simply to use only characters from the bony labyrinth, but the only way to achieve a good phylogenetic tree would include more species than now, since only 26 species are scanned of a family with well over 50 members (Frost, 1991; Gould, 1995, He et al., 2001). In order to get a representative database at least five scans should be made from every genus (preferably every species), as it would allow measuring of intraspecific variation as well as the variation amongst the genera, previously observed in different mammals (Billet et al., 2012; Welkers et al., 2009). The last option to increase the database would be to fill in the gaps of the database made by Gould (1995, 2001). Although the research was well grounded, some very common extant species (e.g., *Atelerix pruneri*, *Echinosorex rafflesi*, *Mesechinus hughi* and *Paraechinus micropus*), as well as fossils were missing. Further completing this database is a simple but effective way to cover all the members of Erinaceidae, allowing the gaps in the database to be filled and giving the fossils a more stable place within the phylogenetic tree.

Conclusion

The topology in the phylogenetic trees that are obtained using only bony labyrinth characters (Figures 18 and 19) shows a reliable resolution of species (at least at genus level) and suggests that the variation across genera for the inner ear in Erinaceidae is a trustworthy characteristic, in accordance with previous findings on other mammals (Macrini et al., 2010; Malinzak et al., 2012). Unfortunately, right now there is too little information to examine the variation present within a genus, leaving the area of inter-specific variation for Erinaceinae unexplored. The

addition of new bony labyrinth CT-scans to the already existing database would certainly have a beneficial effect on the still incomplete bony labyrinth database of Erinaceidae, as there remain members of the Erinaceidae family (both extinct and extant) of which the morphology of the bony labyrinth is unknown. When the foundation of inner ear data becomes sturdier both intra-specific and inter-specific variation can be compared, including their influence on the position of species in a phylogenetic tree based on bony labyrinth characters only. Earlier work (Billet et al., 2012) showed the importance of correcting for the possibility of great variation within a genus, which was not considered during this project, since most species available were only represented by one scan. At present state, the lack of correction could be the reason why some species (e.g. *Mesechinus dauuricus*) behaved unexpectedly depending on the data used in the phylogenetic analysis. So does the position *Mesechinus dauuricus* shifts from within the Erinaceini group when a combination of datasets is used to a branch in the Galericinae clade (Figure 20 until 22) when only the characters of the bony labyrinth are used (Figure 18 and 19).

When searching for the optimal phylogenetic tree, the inclusion of fossils seems to be equally important as the adding of more data, since it could help with identifying which characters could be an acquisition of characters over an evolutionary time. The characteristics of a fossil with a morphology intermediate between the Erinaceinae and Galericinae clade (e.g. *Galerix* in Figure 19 and 22) could be a great guide as to which character states are primitive, while other characters from fossils are shared with much more derived species (e.g. *Parasorex* and *Postpalerinaceus* in Figure 19). The more species are examined in order to arrange the series the better, since it will exclude inaccurate matrix determinations

by correcting the deviation by the number of specimens analysed.

Acknowledgements

This project was funded by the Leidse Universiter fonds, the Minerva scholarship foundation, the Erasmus mobility grant, the Leidse Outbound, the Jo Kolk foundation, the Institut Biology Leiden travel fund and the Synthesis grant. The author is indebted to Dr. Lars van den Hoek Ostende (Naturalis Biodiversity Centre, Leiden) and Dr. Robert Asher (University Museum of Zoology, Cambridge) for co-hosting and supervising the research project, Dr. Pablo Peláez-Campomanes (Museo Nacional de Ciencias Naturales, Madrid) for providing and preparing *Parasorex* and *Postpalerinaceus* material, Dirk van der Marel (Naturalis Biodiversity Centre, Leiden) for learning me how to use the scanning equipment, Pepijn Kamminga (Naturalis Biodiversity Center, Leiden), Martin Rucklin (Naturalis Biodiversity Center, Leiden and Nick Crumpton (University Museum of Zoology, Cambridge) all introducing me to different types of 3D reconstruction software, Rick Thompson (University Museum of Zoology, Cambridge) for his help with Paup while conducting phylogenetic trees, Rachel O'Meara (University Museum of Zoology, Cambridge) and Eline Sikkema (Univeristy Leiden) for their linguistic improvements on the paper. I am gratefull to the many museums, who helped to facilitate this research and without the generous sharing of the Erinaceidae collection from the National Biodiversity Center, University Museum of Zoology, Museo Nacional de Ciencias Naturales, Naturhistorisches Museum Basel, Naturhistorische Museum Wien and the Museum für Naturkunde this paper could not have been realized.

References

- Abate, A. F., Nappi, m., Ricciardi, S. and Tortora, G. 2003. Faces: 3D Facial reconstruction from ancient Skulls using content based image retrieval. *Journal of visual languages and computing* **15**: 373-389.
- Baudelot, S. 1972. Étude des Chioptères, Insectivores et Rongeurs du Miocène de Sansa (Gers.). *Tesis Doctoral, Universidad Paul Sabatier du Toulouse*: 1-364.
- Billet, G., Hautier, L., Asher, R. J., Schwarz, C., Crumpton, N. and Martin, T. 2012. High morphological variation of vestibular system accompanies slow and infrequent locomotion in three-toed sloths. *Proceedings of the royal society biology* **279**: 3932-3939.
- Braun, E. L. and Kimball, R. T. 2002. Examining basal avian divergences with mitochondrial sequences: model complexity, taxon sampling, and sequence length. *Systems Biology* 614-625.
- Butler, R. M. 1956. Erinaceidae from the Miocene of east Africa. *British Museum (natural history) fossil mammals Africa* **11**: 1-75.
- Butler, P. M. 1980. The giant erinaceid insectivore, *Deinogalerix* Freudenthal, from the upper Miocene of Gargano, Italy. *Scripta geologica* **57**: 1-72.
- Butler, P., M. 1984. Macroscelidea, Insectivora and Chiroptera from the Miocene of east Africa. *Palaeovertebrata (Montpellier)* **14**: 117-200.
- Corbet, G. B. 1988. The family Erinaceidae: a synthesis of its taxonomy, phylogeny, ecology and zoogeography. *Mammal review* **18**: 117-172.
- Cox, P. G. and Jeffery, N. 2010. Semicircular canals and agility: the influence of size and shape measures. *Journal of anatomy* **216**: 37-47.
- Donoghue, M. J., Doyle, J. A., Gauthier, J., Kluge, A. G. and Rowe, T. 1989. The importance of fossils in phylogeny reconstruction. *Annual review of ecology and systematic* **20**: 431-460.
- Doukas, C. S. and Hoek Ostende, L.W. van den. 2006. Insectivores (Erinaceomorpha, Soricomorpha; Mammalia) from Karydia and Komotini (Thrace, Greece; MN 4/5). *Beiträge zur paläontologie* **30**: 109-131.
- Ekdale, E. G. 2010. Ontogenetic variation in the bony labyrinth of *Monodelphis domestica* (mammalia: Marsupialia) following ossification of the inner ear cavities. *The anatomical record*, **293**: 1862-1912.
- Ekdale, E. G. 2013. The anatomy of the bony labyrinth (innerear) of placental mammals. *PLoS ONE* **8(6)**: e66624.
- Ekdale, E. G. and Rowe, T. 2011. Morphology and variation within the bony labyrinth of zhelestids (Mammalia, Eutheria) and other therian mammals. *Journal of vertebrate paleontology* **31**: 658 - 675.
- Engesser, B. 1980. Insectivora and Chiroptera (Mammalia) aus dem Neogen der Türkei. *Schweizerische Paläontologische abhandlungen* **102**: 45-149.
- Farke, A. A., Chok, D. J., Herrero, A., Scolieri, B. and Werning, S. 2013. Ontogeny in the tube-crested dinosaur *Parasaurolophus* (Hadrosauridae) and heterochrony in hadrosaurids. *PeerJ*. **182**: DOI 10.7717.
- Fleischer, G. 1973. Studien am Skelett des Gehörorgans der Säugetiere, einschliesslich des Menschen. *Säugetierk. Mitt.* **21**: 131-239.
- Frost, D. R., Wozencraft, W. C. and Hoffmann, R. S. 1991. Phylogenetic relationships of hedgehogs and gymnures (Mammalia, Insectivora, Erinaceidae). *Smithsonian contributions to zoology* **518**: 1-69.
- Gawne, C. E. 2005. The genus *Proterix* (insectivore, Erinaceidae) of the upper Oligocene of North America. *The American museum of natural history* **2314**: 1-26.
- Georgi, J. A., Sipla, J. S. and Forster, C. A. 2013. Turning semicircular canal function on its heels: dinosaurs and a novel vestibular analysis. *PLoS ONE* **8(3)**: e58517.
- Gosselin-Ildari, A. D. 2006. Functional morphology of the bony labyrinth in primates. *B.A. thesis, The university of Texas at Austin*: 1-52.
- Gould, G. C. 1995. Hedgehog phylogeny (Mammalia, Erinaceidae): The reciprocal illumination of the quick and the dead. *American museum novitates* **3131**: 1-45.
- Gould, G. C. 2001. The phylogenetic resolving power of discrete dental morphology among extant hedgehogs and the implications for their fossil record. *American museum novitates* **3340**: 1-52.
- Grantham, T. 2004. The role of fossils in phylogeny reconstruction: Why is it so difficult to integrate paleobiological and neontological evolutionary biology? *Biology and philosophy* **19**: 687-720.

- Gray, A. A. 1906. Observations on the labyrinth of certain animals. *Proceedings of the royal society biology* **78**: 284-296.
- Gray, A. A. 1907. The labyrinth of animals, Vol 1. London: Churchill.
- Gray, A. A. 1908. The labyrinth of animals, Vol 2. London: Churchill.
- Gunz, P., Ramsier, M., Kuhrig, M., Hublin, J. and Spoor, F. 2012. The mammalian bony labyrinth reconsidered, introducing a comprehensive geometric morphometric approach. *Journal of anatomy* **220**: 529-543.
- He, K., Chen, J., Gould, G. C., Yamaguchi, N., Ai, H., Wang, Y., Zhang, Y. and Jiang, Y. 2012. An estimation of Erinaceidae phylogeny: A combined analysis approach. *PLoS ONE* **7**(6): 39304.
- Heaney, L. R. and Morgan, G. S. 1982. A new species of gymnure, *Podogymnura*, (Mammalia, Erinaceidae), from Dinagat Island, Philippines. *Proceedings of the biological society of Washington* **95**: 13-26.
- Hoek Ostende, L. W. van den. 2001. A revised generic classification of the Galericiini (Insectivora, Mammalia) with some remarks on their palaeogeography and phylogeny. *Geobios* **34**(6): 681-695.
- Hyrtil, J. 1845. Vergleichend-anatomische Untersuchungen über das innere Gehörorgan des Menschen und der Säugethiere: Mit neun Kupfertafeln
- Jeffery, N. and Spoor, F. 2004. Prenatal growth and development of the modern human labyrinth. *Journal of anatomy* **204**: 71-92.
- Jones, G. M. and Spells, K. E. 1963. A theoretical and comparative study of the functional dependence of the semicircular canal upon its physical dimensions. *Proceedings of the royal society biology* **157**: 403-419.
- Leche, W. 1902. Zur Entwicklungsgeschichte des Zahnsystems der Säugethiere. Zugleich ein Beitrag zur stammesgeschichte dieser Thiergruppe. 2 Theil, phylogenie 1 Heft. Die familie der Erinaceidae. *Zoologica, Stuttgart* **15**: 103.
- Leche, W. 1920. Morphologische-geographische formenreihen bei den Säugethieren. *Acta Universitatis lundensis* **16**.
- Macrini, T. E., Flynn, J. J., Croft, D. A. and Wyss, A. R. 2010. Inner ear of a notoungulate placental mammal: anatomical description and examination of potentially phylogenetically informative characters. *Journal of anatomy* **216**: 600-610.
- Malinzak, M. D., Kay, R. F. and Hullar, T. E. 2012. Locomotor head movements and semicircular canal morphology in primates. *PNAS* **109** (44): 17914-14919.
- Marugán-Lobón, J., Chiappe, J. M. and Farke, A. A. 2013. The variability of inner ear orientation in saurischian dinosaurs: testing the use of semicircular canals as a reference system for comparative anatomy *PeerJ* **124**: DOI10.7717.
- Mathew, W. D. and Mook, C. C. 1933. New fossil mammals from the deep river beds of Montana. *America museum novitates* **601**: 107.
- Mckenna, M. C. and Holton, C. P. 1967. A new insectivore from the Oligocene of Mongolia and a new subfamily of hedgehogs. *The American museum of natural history* **2311**: 1-11.
- Meade, G. E. 1941. A new erinaceid from the lower Miocene. Geological series of *field museum of natural history* **8** (7): 43-47.
- Meng, J. and Fox, R. C. 1995. Osseous inner ear structures and hearing in early marsupials and placentals. *Zoological Journal of the Linnean Society* **115**: 47-71.
- Morgan, G. S. and Ottenwalder, J. A. 1993. A new extinct species of *Solenodon* (Mammalia:Insectivora:Solenodontidae) from the late Quaternary of Cuba. *Annals of Carnegie museum* **62** (2): 151-164.
- Novacek, M. J., Bown, T. M. and Schankler, D. 1985. On the classification of the early tertiary Erinaceomorpha (Insectivora, Mammalia). *American museum novitates* **2813**: 1-22.
- Nowak, R. M. and Paradiso, J. L. 1983. Walker's Mammals of the World Vol. 1, 4th edition. *Johns Hopkins university press, Baltimore & London*.
- Pacholke, H. D., Amdur, R. J. Schmalfluss, I. M., Louis, D. and Mendenhall, W. M. 2005. Contouring the middle and inner ear on radiotherapy planning scans. *American journal of clinical oncology* **28**(2): 143-147.
- Patterson, C. 1981. Significance of Fossils in Determining Evolutionary Relationships. *Annual review of ecology and systematics* **12**: 195-223.

- Prieto-Márquez, A. and Wagner, J. R. 2013. The “Unicorn” dinosaur that wasn’t: A new reconstruction of the crest of *Tsintaosaurus* and the early evolution of the lambeosaurine crest and rostrum. *PLoS ONE* **8** (11): e82268.
- Prieto, J., Hoek Ostende, L. W. van den and Bohme, M. 2011. Reappearance of *Galerix* (Erinaceomorpha, Mammalia) at the limit middle/upper Miocene in south Germany: biostratigraphical and paleoecological implications. *Contributions to zoology* **80**(3): 179–189.
- Prieto, J., Hoek Ostende, L.W. van den and Janos, H. 2012. The Middle Miocene insectivores from Sámsonháza 3 (Hungary, Nógrád County): Biostratigraphical and palaeoenvironmental notes near to the Middle Miocene Cooling. *Bulletin of geosciences* **87**: 227–240.
- Rich, T. H. V. 1981. Origin and history of the Erinaceinae and Brachyericinae (Mammalia, Insectivora) in North America. *Bulletin of the American museum of natural history* **17**: 1–116.
- Roca, A. L., Bar-Gal, G.K., Eizirik, E., Helgen, K. M., Maria, R., Springer, M. S., O’Brien, S. J. and Murphy, W. J. 2004. Mesozoic origin for West Indian insectivores. *Nature* **429**: 649–651.
- Schmelzle, T., Sanchez-Villagra, M. R. and Maier, W. 2007. Vestibular labyrinth diversity in diprotodontian marsupial mammals. *Mammal study* **32**: 83–97.
- Smith, A.B. 1998. What does Palaeontology Contribute to Systematics in a Molecular World. *Molecular phylogenetics and evolution* **9**: 437–447.
- Spoor, F. and Zonneveld, F. 1995. Morphometry of the primate bony labyrinth: a new method based on high-resolution computed tomography. *Journal of anatomy* **186**: 271–286.
- Spoor, F. and Zonneveld, F. 1998. Comparative review of the human bony labyrinth. *Yearbook of physical anthropology* **41**: 211–251.
- Stieger, C., Djerić, D., Kompis, M., Remonda, L. and Hausler, R. 2006. Anatomical study of the human middle ear for the design of implantable hearing aids. *Auris nasus larynx* **4**: 375–380.
- Sulimski, A. 1970. On some Oligocene insectivore remains from Mongolia. *Palaeontologica Polonica* **21**: 53–70.
- Swofford, D. L. 2003. PAUP*: Phylogenetic Analysis Using Parsimony (* and Other Methods), *Sinauer Associates* **4.0b** (10).
- Van Valen, L. 1967. New Palaeocene insectivores and insectivore classification. *Bulletin of the American museum of natural history* **135**: 219–284.
- Viret, J. 1938. Étude sur quelques Erinacéidés fossils spécialement sur le genre *Palerinaceus*. *Travaux du Laboratoire de Géologie de la Faculté des Sciences de Lyon*. **34** (28): 1–32.
- Villier, B. and Carnevale, G. 2013. A new skeleton of the giant hedgehog *Deinogalerix* from the Miocene southern Italy. *Journal of vertebrate paleontology* **33** (4): 902–923.
- Villier, B., Vos, J. de and Hoek Ostende, L. W. van den. 2013. New discoveries on the giant hedgehog *Deinogalerix* from the Miocene of Gargano (Apulia, Italy). *Geobios* **46**: 63–75.
- Welker, K. L., Orkin, J. D. and Ryan, R. M. 2009. Analysis of intraindividual and intraspecific variation in semicircular canal dimensions using high-resolution x-ray computed tomography. *Journal of anatomy* **215**: 444–451.
- Werner, C. F. 1933. Das Ohrlabrynth der Tiere. *Passow-schafer beitrage* **30**: 390–408.
- West, C. D. 1985. The relationship of the spiral turns of the cochlea and the length of the basilar membrane to the range of audible frequencies in ground dwelling mammals. *Journal of the acoustical society of America* **77**: 1091–1101.
- Zander, R. H. 2004. Bootstrap and Jackknife proportions, decay index, and Bayesian posterior probability. *Phyloinformatics* **2**: 1–13.
- Ziegler, R. 2005. Erinaceidae and Dimylidae (Lipotyphla) from the upper middle Miocene of south Germany. *Senckenbergiana lethaea* **85**: 131–152.
- Ziegler, R. 2005. The insectivores (Erinaceomorpha and Soricomorpha, mammalia) from the Late Miocene homocoid locality Rudabánya. *Palaeontographia Italica* **90**: 53–81.
- Ziegler, R. and Daxner-Höck, G. 2005. Austria. *Scripta geology special* **5**.
- Ziegler, R., Dahlmann, T. and Storch, G. 2007. Oligocene-Miocene vertebrates from the valley of lakes (central Mongolia): morphology, phylogenetic and stratigraphic implications. *Annalen des naturhistorische museums in Wien* **108** A: 53–164.

Appendix

Table 1 Specimens reviewed in a combination of bony labyrinth analyses and previously made matrixes

Abbreviations: AMNH=American Museum of Natural History; F:AM=Frick Collection, American Museum of Natural History; BM=British Museum (Natural History); MNCN=Museo Nacional de Ciencias Naturalis; MNHP=Museum National D'Histoire Naturelle; NBC=National Biodiversity Center; NMB=Naturhistorisches Museum Basel; NMW=Naturhistorische Museum Wien; UCMP=University of California Museum of Paleontology; UMZC=University Museum of Zoology Cambridge; USNM=United States National Museum (Smithsonian Institution); ZMB=Museum für Naturkunde. Specimens that do not have a number are indicated with XXX.

	Innerear data		Gould, 1995				Gould, 2001					
Species	Museum	Number	Museum	Number	Museum	Number	Museum	Number	Museum	Number	Museum	Number
<i>Amphechinus edwardsi</i>	NMB	SAUS_1										
<i>Amphechinus Paleaoedwardsi</i>	NMB	SAU_632										
<i>Atelerix albiventris</i>	NBC	RMNH.MA M.2518	AMNH	16581			USNM	378723	USNM	378741	USNM	402180
			AMNH	210285			USNM	378725	USNM	378742	USNM	402181
			USNM	181442			USNM	378726	USNM	378746	USNM	402182
							USNM	378728	USNM	378747	USNM	402183
							USNM	378729	USNM	378748	USNM	402184
							USNM	378730	USNM	378750	USNM	375927
							USNM	378731	USNM	378751	USNM	375928
							USNM	378740	USNM	402179		
<i>Atelerix algirus</i>	NBC	RMNH.MA M.18759	AMNH	31247			USNM	476050	USNM	476057	USNM	476064
			USNM	476058			USNM	476051	USNM	476058	USNM	476065
							USNM	476052	USNM	476059	USNM	476066
							USNM	476053	USNM	476060	USNM	470578
							USNM	476054	USNM	476061	USNM	470579
							USNM	476055	USNM	476062	USNM	482681
							USNM	476056	USNM	476063	USNM	140766
<i>Atelerix frontalis</i>	NBC	RMNH.MA M.980	AMNH	87639	AMNH	207247						
			AMNH	87640	USNM	267653						
<i>Atelerix pruneri</i>	ZMB	MfN.60577										
<i>Atelerix sclateri</i>			???	???								

<i>Brachyerix macrotis</i>			AMNH	21335	F:AM	76695						
			F:AM	74965	AMNH	21335						
			F:AM	74964								
<i>Echinosorex gymnurus</i>	NBC	RMNH.MA M.5061	AMNH	102781	BM	55.12.24.35	USNM	487885	USNM	487900	USNM	145584
	NMB	NMBC_3745	AMNH	102782	BM	60.5.14.73	USNM	487887	USNM	487902	USNM	145585
	ZMB	MfN.72229	AMNH	103736	BM	14.12.8.104	USNM	487888	USNM	487903	USNM	145586
			AMNH	103737	BM	91.10.7.45	USNM	487889	USNM	283474		
			AMNH	103883	BM	0.3.30.31	USNM	487890	USNM	115489		
			AMNH	103886	BM	8.7.1.7.9	USNM	487891	USNM	357885		
			AMNH	106068	BM	51.181	USNM	487892	USNM	3787		
			AMNH	106069	BM	12.24.90	USNM	487893	USNM	357886		
			BM	34698	BM	551.453	USNM	487894	USNM	357888		
			BM	76.5.2.7	BM	51.180	USNM	487895	USNM	487886		
			BM	87.178	BM	14.12.8.102	USNM	487896	USNM	357887		
			BM	87.179	BM	611.157	USNM	487897	USNM	83704		
			BM	6.10.4.13	USNM	487891	USNM	487898	USNM	145581		
			BM	712.613			USNM	487899	USNM	145582		
<i>Echinosorex rafflesi</i>	UMZC	E5111B										
<i>Erinaceus amurensis</i>							USNM	176251	USNM	239591	USNM	270542
							USNM	199681	USNM	239592	USNM	240325
							USNM	239770	USNM	197779	USNM	252158
							USNM	239590	USNM	270541		
<i>Erinaceus concolor</i>	NBC	ZMA.MAM. 24943	AMNH	149412	USNM	369533						
	ZMB.	MfN 36934										
<i>Erinaceus europaeus</i>	NMB	7008	AMNH	35304			USNM	153409	USNM	251765	USNM	86923
	NBC	ZMA.MAM. 86/4	AMNH	10735			USNM	153410	USNM	251766	USNM	36034(20807)

			USNM	153410			USNM	153411	USNM	251767	USNM	174660
							USNM	153412	USNM	251768	USNM	794
							USNM	1856	USNM	271142	USNM	795
<i>Galerix exilis</i>	NMW	XXX										
<i>Galerix</i> sp.			AMNH	10516 A-H	BM	M5380						
			BM	M4845	BM	M5383						
<i>Hemiechinus auritus</i>	NBC	ZMA.MAM.1765	AMNH	22876			AMNH	203197	AMNH	244380	AMNH	57222
			AMNH	22889			AMNH	203198	AMNH	244280	AMNH	84001
			USNM	340933			AMNH	203199	AMNH	176282	AMNH	31246
			BM	80021			AMNH	203200	AMNH	87085	AMNH	184065
							AMNH	170226	AMNH	85309	AMNH	22876
							AMNH	170227	AMNH	85308	AMNH	22889
							AMNH	170228	AMNH	31248	AMNH	80021
							AMNH	170229	AMNH	57216		
							AMNH	244379	AMNH	57217		
<i>Hemiechinus collaris</i>			???	XXX								
<i>Hylomys parvus</i>	NBC	RMNH.MA.M.38335	BM	19.11.5.8								
			BM	19.11.5.9								
			BM	19.11.5.10								
			BM	19.11.5.11								
<i>Hylomys suillus</i>	ZMB	MfN.48724					USNM	481278	USNM	481285	USNM	521659
	NBC	ZMA.MAM.29225					USNM	481279	USNM	481286	USNM	521660
							USNM	481280	USNM	481287	USNM	521661
							USNM	481281	USNM	481288	USNM	155660
							USNM	481283	USNM	481289		
							USNM	481284	USNM	481290		
<i>Hylomys s.dorsalis</i>	NBC	RMNH.MA.M.38344	USNM	292347	BM	712617						
			BM	55.66.1	BM	712618						
			BM	712614	BM	92.9.64						
			BM	712615	BM	95.10.4.3						
			BM	712616	BM	95.10.4.4						

<i>Hylomys s. maxi</i>	NBC	RMNH.MA M.38348	BM	62.711	BM	71.26.17						
			BM	71.26.14	BM	71.26.18						
<i>Hylomys s. pegunensis</i>	NBC	RMNH.MA M.12683										
<i>Hylomys s. siamensis</i>			BM	2610439	BM	2610436						
<i>Hylomys s. suillus</i>	NBC	RMNH.MA M.38349										
<i>Lanthanotherium sp</i>			BM	M16335	UCMP	82731						
			UCMP	54600								
<i>Mesechinus dauuricus</i>	NMB	9110	USNM	270539								
<i>Mesechinus hughi</i>												
<i>Metechinus sp</i>			F:AM	74925	F:AM	76707						
			F:AM	76698								
<i>Mioechinus sp</i>			F:AM	74925								
<i>Neohylomys hainanensis</i>			???	XXX								
<i>Neotetracus sinensis</i>	NMB	XXX	USNM	241402	BM	11.8.61	AMNH	115505	AMNH	115516	AMNH	44248
			BM	11.2.1.21	BM	11.2.1.19	AMNH	115506	AMNH	115517	AMNH	44249
			BM	11.2.1.22			AMNH	115508	AMNH	115518	AMNH	44267
			BM	82.205			AMNH	115509	AMNH	115519	AMNH	44268
			BM	33.4.1.117			AMNH	115510	AMNH	115520	AMNH	44270
			BM	33.4.1.124			AMNH	115511	AMNH	115522	AMNH	44271
			BM	33.4.1.132			AMNH	115512	AMNH	115523	AMNH	57199
			BM	11.2.1.15			AMNH	115514	AMNH	115524		
			BM	11.2.1.18			AMNH	115515	AMNH	115525		
<i>Neurogymnurus sp.</i>	NMB	QH391	BM	M7509	MNHN	QU8692						
			BM	M9653	MNHN	QU8693						
			BM	M9655	MNHN	QU8694						
			BM	M2388	MNHN	QU8695						

			BM	9654	MNHN	QU8697						
			BM	5109	MNHN	QU8698						
			MNHN	QU8680	MNHN	QU1070						
			MNHN	QU8691								
<i>Paraechinus aethiopicus</i>	NBC	ZMA.MAM.15047	USNM	470566			USNM	311732	USNM	384832	USNM	470568
							USNM	311737	USNM	410872	USNM	470569
							USNM	311738	USNM	410873	USNM	476067
							USNM	311739	USNM	482512	USNM	476068
							USNM	311740	USNM	470563	USNM	476069
							USNM	321572	USNM	470564	USNM	482862
							USNM	325906	USNM	470565	USNM	482863
							USNM	325907	USNM	470566		
							USNM	325908	USNM	470567		
<i>Paraechinus hypomelas</i>	NMW	15242	USNM	326697			USNM	326695	USNM	326701	USNM	368934
							USNM	326696	USNM	327913	USNM	368935
							USNM	326697	USNM	327915	USNM	368936
							USNM	326698	USNM	352951	USNM	368937
							USNM	326699	USNM	368931	USNM	410929
							USNM	327914	USNM	368932		
							USNM	326700	USNM	368933		
<i>Paraechinus micropus</i>	NMW	15243										
<i>Parasorex</i> sp.	MNCN	Bat-1-2002-C7-12										
<i>Podogymnura aureospinula</i>			???	???								
<i>Podogymnura truei</i>			BM	53.660	BM	65.660						
			BM	53.659	AMNH	XXX						
<i>Postpalerinaceus</i> sp.	MNCN	B-1051										

	MNCN	Bat-1-2002-C7-34										
<i>Ancestor</i>			Unknown	XXX								
<i>Leptictids</i>			F:AM	108194								
			AMNH	62369								
<i>Tenrecoids</i>	UMZC	E5450B	AMNH	17060	AMNH	100749						
			AMNH	170601	AMNH	170538						
			AMNH	31261	AMNH	170540						
			AMNH	31257	AMNH	100762						
			AMNH	120250	AMNH	170512						
			AMNH	240968	AMNH	100733						
<i>Soricoids</i>			AMNH	3830	AMNH	114825						
			AMNH	82484	AMNH	44758						
			AMNH	168050	AMNH	70790						
			AMNH	240937	AMNH	42558						
			AMNH	180969	AMNH	160455						
			AMNH	48455	AMNH	110591						
			AMNH	114844								
<i>Talpa sp</i>	UMZC	E.5334N										
<i>Solenodon cubanus</i>	UMZC	E5418B										

Table 2 Characteristics as specified by Gould (1995, 2001)

Only a selection of both was used in order to prevent overlap. The numbers of the characteristics used in this matrix are described below.

	Characteristics	Total
Gould, 1995	1-62, 64-103	102
Gould, 2001	4-6, 8, 10, 24, 27, 28, 32, 39, 42, 43, 46, 47, 54-57, 67-69, 72, 77, 78, 88, 93-96, 99, 105, 106, 109, 111, 117, 121, 133-135, 142-145, 147, 149-153, 160, 161, 163, 164, 172, 173, 175-181, 183, 185, 189, 191, 195, 196, 198, 205-210, 219, 220, 222, 223, 225, 226, 228, 229, 233-238, 240, 241, 243-245, 248	95
Total		197

Table 3 The used DNA material from GENbank, ordered by species

In total three different parts of the genome were used: 12S, CytB and NADH. When the sequence was available on the GenBank for any of them, it is marked as a “Yes” in the table. In cases where the site was not sequenced, this was marked as a “No.”

Species	12S	CytB	NADH
<i>Atelerix albiventris</i>	Yes	No	No
<i>Echinosorex gymnurus</i>	Yes	No	Yes
<i>Erinaceus amurensis</i>	Yes	Yes	Yes
<i>Erinaceus concolor</i>	Yes	No	No
<i>Erinaceus europaeus</i>	Yes	Yes	Yes
<i>Hemiechinus auritus</i>	Yes	Yes	Yes
<i>Hylomys parvus</i>	No	Yes	No
<i>Hylomys suillus</i>	Yes	Yes	Yes
<i>Hylomys s.dorsalis</i>	No	Yes	No
<i>Hylomys s. maxi</i>	No	Yes	No
<i>Hyloms s. microtinus</i>	No	Yes	No
<i>Hylomys s. siamensis</i>	No	Yes	No
<i>Hylomys s. suillus</i>	No	Yes	No
<i>Mesechinus dauuricus</i>	Yes	Yes	Yes
<i>Mesechinus hughi</i>	Yes	Yes	Yes
<i>Neohylomys hainansis</i>	Yes	Yes	Yes
<i>Neotetracus sinensis</i>	Yes	Yes	Yes
<i>Paraechinus aethiopicus</i>	Yes	Yes	Yes
<i>Podogymnura truei</i>	Yes	Yes	Yes
<i>Talpa sp</i>	Yes	Yes	No
<i>Solenodon cubanus</i>	Yes	No	No

Table 4 The data matrix of the 25 Bony labyrinth characters

The characters can have two to four different character states.

Species	1	2	3	4	5	6	7	8	9	10	11	12	13	14	15	16	17	18	19	20	21	22	23	24	25
<i>Amphechinus edwardsi</i>	1	2	1	1	1	2	0	0	1	1	1	1	1	1	0	1	2	1	1	2	2	0	2	2	1
<i>Amphechinus Palaeoerinaceus edwardsi</i>	1	2	2	1	2	3	0	1	0	1	1	1	0	2	0	1	2	1	2	2	2	1	2	1	1
<i>Atelerix algirus</i>	1	1	1	0	0	1	0	1	1	1	0	1	0	0	0	2	0	1	2	0	2	2	1	1	0
<i>Atelerix frontalis</i>	1	1	2	0	1	3	1	0	1	0	1	1	0	1	1	1	2	1	0	2	2	0	0	1	0
<i>Atelerix pruneri</i>	1	1	0	0	1	1	1	0	1	1	1	1	0	0	0	2	1	1	2	1	2	2	1	1	0
<i>Echinosorex gymnurus</i>	1	3	1,2	2	0,1	2	0	1	0	2,3	0,1	1	0,1	0,1	0,1	1	2	1	2	2	2	1	2,3	2,3	1,2
<i>Echinosorex rafflesi</i>	1	3	1	2	0	1	0	1	0	2	1	1	0	1	0	0	2	1	1	0	0	1	1	1	1
<i>Erinaceus albiventris</i>	1	3	1	0	0	2	1	0	1	1	1	1	0	1	0	2	1	2	3	1	2	2	1	1	0
<i>Erinaceus concolor</i>	0,1	1	2	0	0,1	1,2	0	0	1	1	1	1	1	1	0,1	1,2	2	1	2	2	2	2	1	1	0
<i>Erinaceus europaeus</i>	1	0,1	2	0	1	2	0	0,1	1	0,1	0	1	1	0,1	0,1	2	2	1	2	2	2	2	1	1	0
<i>Galerix exilis</i>	1	3	2	2	1	1	0	1	0	2	1	1	1	1	0	2	2	1	1	2	2	0	1	1	1
<i>Hemiechinus auritus</i>	0	1	1	1	1	2	1	0	1	1	1	1	2	0	1	2	2	1	0	2	2	1	1	1	0
<i>Hylomys parvus</i>	2	2	1	2	1	2	0	2	0	2	1	0	0	1	0	2	2	1	2	2	2	1	1	2	1
<i>Hylomys suillus</i>	1,3	2,3	1,2	2	1	1,2	0	1,2	0	2	1	0,1	1	1	0,1	3	2	1,2	1,2	2	1,2	0,2	1,2	2	1
<i>Hylomys s. dorsalis</i>	1	2	0	2	0	1	0	2	0	1	1	1	0	1	0	2	2	1	2	2	2	1	2	2	1
<i>Hylomys s. maxi</i>	1	2	1	2	1	3	0	2	0	2	1	0	1	1	0	2	2	1	1	2	2	1	2	3	1
<i>Hylomys s. peguensis</i>	1	3	2	2	1	1	0	2	0	2	1	0	1	1	1	2	2	1	2	2	2	2	2	2	1
<i>Hylomys s. suillus</i>	2	2	1	2	1	2	0	1	0	2	1	1	0	1	0	2	2	2	2	2	2	2	2	2	1
<i>Mesechinus dauricus</i>	1	1	1	0	0	1	0	0	0	2	0	1	2	1	0	1	2	1	1	2	2	1	1	1	0
<i>Neotetracus sinensis</i>	1	2	1	2	0	2	0	2	0	2	1	0	0	1	0	2	3	2	2	2	2	1	1	2	1
<i>Neurogymnurus sp.</i>	1	3	2	1	1	1	0	1	0	2	0	2	1	1	1	1	2	1	2	2	2	1	3	2	3
<i>Paraechinus aethiopicus</i>	1	1	0	1	1	2	1	0	1	1	1	0	1	0	1	2	2	1	0	2	2	0	0	1	0
<i>Paraechinus hypomelas</i>	0	1	1	1	0	3	0	1	0	2	1	1	1	2	0	2	3	3	2	2	2	2	0	0	0
<i>Paraechinus micropus</i>	0	?	0	1	1	1	1	0	1	1	0	2	1	1	0	2	2	0	0	2	1	1	0	0	0

<i>Parasorex</i> sp.	2	?	2	1	1	0	0	2	1	1	1	1	0	2	0	2	2	1	0	2	2	1	1	1	0
<i>Postpalerinaceous</i> sp.	1,2	?	1	1	1,2	2	0	1	0	2	0	2	0	2	0	1,2	2	1	1	2	2	1	1	?	0
<i>Setifer setosus</i>	0	2	1	1	0	1	0	1	0	2	0	2	0	0	0	2	2	1	2	1	2	2	2	1	1
<i>Solenodon cubanus</i>	0	2	0	2	0	2	0	1	0	2	0	2	1	1	1	2	2	1	2	2	2	2	1	1	0
<i>Talpa europaea</i>	?	?	?	2	2	2	?	?	?	?	0	2	?	?	?	?	?	?	?	?	?	?	?	?	1

